

Surface effects on magnetic phase transitions

K. Binder*

Physik Department E14, TUM, 8046 Garching-bei-München, West Germany

P. C. Hohenberg

Bell Laboratories, Murray Hill, New Jersey 07974

(Received 10 August 1973)

The surface scaling theory previously presented by the authors is developed further, and derived heuristically from a cluster model. Monte Carlo calculations are carried out to obtain the spatial and temperature dependence of the magnetization in Ising and Heisenberg systems with free surfaces. The exponent β_1 of the (surface) layer magnetization is shown to agree with the scaling value ($\beta_1 \approx 2/3$) previously derived. In the Heisenberg system, the results at low temperature agree with a spin-wave calculation by Mills and Maradudin. Ising models with modified exchange $J_s = J(1+\Delta) \neq J$ on the surface are considered, both in mean-field theory and by means of high-temperature-series expansions. The critical value Δ_c for surface ordering is found from the series to be 0.6, compared to the mean-field value of 0.25. For $\Delta > \Delta_c$ there is a temperature region in which the surface behaves like a bulk two-dimensional Ising model near its phase transition. The critical exponents experience a crossover at $\Delta = \Delta_c$, which is reflected in poorly behaved series, and effective exponents differing from the true ones for $\Delta \lesssim \Delta_c$. In the case of weakened surface exchange ($0 < J_s < J$), the layer magnetization is shown to fit a linear temperature dependence over a large temperature range below T_c , thus providing a possible explanation for previous experiments. For sufficiently strong negative J_s , mean-field theory predicts that the surface will order antiferromagnetically while the bulk is ferromagnetic.

I. INTRODUCTION

In a previous paper¹ (hereafter referred to as I) the authors presented a theory of phase transitions in Ising models with free surfaces, and made a number of exponent predictions based on high-temperature-series expansions and scaling relations. The scaling theory of I was subsequently reformulated and extended by Barber.² Some of the exponent predictions made in I, such as that for β_1 , the magnetization on the surface layer, are, in principle, susceptible to experimental measurement,^{3,4} and to direct series evaluation.^{2,5} Since preliminary results^{2,4} indicated a value $\beta_1 \approx 1$, in disagreement with the scaling prediction $\beta_1 \approx \frac{2}{3}$, it seemed worthwhile to reexamine the scaling theory critically, and in particular to determine how sensitive its predictions are to modifications in the model. One such modification, which is of interest in its own right, is to assume that the spins in the free surface interact among one another with an exchange energy J_s which is different^{3,4} from the bulk exchange J . It was observed earlier by Mills,³ on the basis of mean-field theory, that for J_s above a critical value $J_{s,c}$, the system would order on the surface before it ordered in the bulk. As we shall see below, such a situation is particularly interesting since it would lead to the possibility of realizing experimentally a rather ideal two-dimensional system. In Mills's original discussion of this effect,³ he expressed doubts on the applicability of mean-field theory to such a delicate question, and it seemed to us worthwhile to study it with more reliable methods. Moreover, even within mean-field theory, doubts were expressed⁶ on the validity

of Mills's prediction, but as we shall see below, and as has been remarked by Mills,⁷ these doubts are unfounded.

From our study of these more general Hamiltonians, and also of Heisenberg and spherical models, we conclude that the theory presented in I has quite general applicability. Moreover, we find that the phenomenon of surface ordering is not restricted to the mean-field approximation, since it follows also from our series expansions. The main difference between the two methods is that the series yield a critical value $J_{s,c} \approx 1.6J$, which is higher than the mean-field value $J_{s,c} = 1.25J$. For $J_s < J_{s,c}$, the surface orders when the bulk does, and it has the "surface exponents" described in I. For $J > J_{s,c}$ the surface orders at a temperature $T_c(J_s)$ which is higher than the bulk T_c , ($T_{c,b}$) and for $T_{c,b} < T < T_c(J_s)$ the magnetization decays exponentially⁸ into the bulk with a characteristic length equal to the bulk correlation length ξ_b (see Fig. 1). In this temperature region the critical exponents are those of the two-dimensional [or more generally ($d-1$)-dimensional] model. The essential difference between the predictions of the mean-field theory and the series evaluations is in the values of $T_c(J_s)$ and of the critical exponents.

One important technical point which should be mentioned is that the exponents which arise out of the series seem to vary continuously with J_s in the range $J_s < J_{s,c}$. This unphysical behavior for the layer susceptibility exponent γ_1 , for instance, may be explained as arising from the crossover between the "surface" value $\gamma_1 \approx \frac{7}{8}$ for $J_s < J_{s,c}$, and the bulk two-dimensional value $\gamma_1 = \gamma_b^{2d} = \frac{7}{4}$ for $J_s \geq J_{s,c}$. On the other hand, our only information on the correct

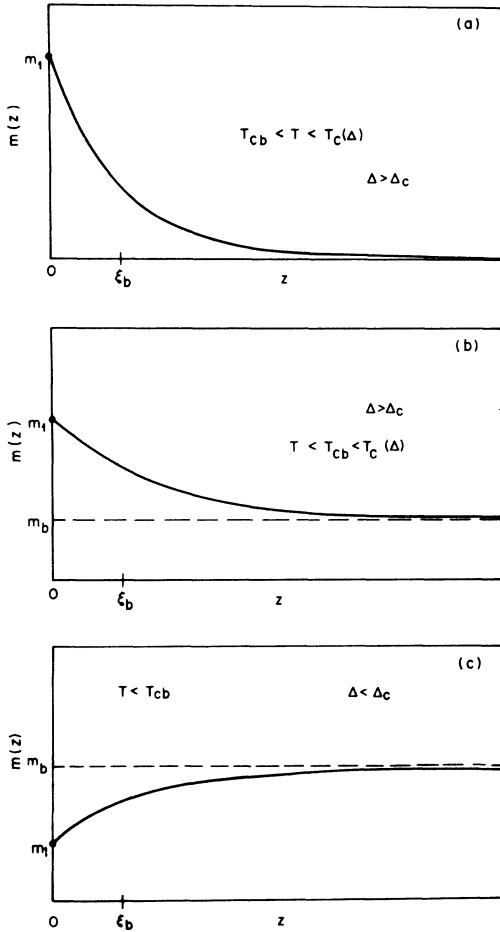


FIG. 1. Schematic diagram of the magnetization as a function of distance from the surface, placed at $z=0$. The exchange at the surface is $J_s = J(1 + \Delta)$, where J is the bulk exchange. There is a critical value Δ_c above which the surface orders before the bulk [part (a)], and the magnetization decays exponentially into the bulk, with a characteristic length equal to the bulk correlation length ξ_b . For $T < T_{cb}$ [part (b)], the magnetization reaches its finite bulk value at large z . For $\Delta < \Delta_c$ [part (c)] the surface only orders when the bulk does, and $m(z)$ is smaller at the surface than in the bulk.

value of γ_1 for $J_s < J_{sc}$ comes from series expansions, and the question naturally arises as to why the series for $J_s = J$ derived in I should itself be considered reliable. We have made a detailed study of both the series results and the mean-field approximation, and our conclusion is that the series are indeed more reliable for $J_s \approx J$, than for $J < J_s \lesssim J_{sc}$, so that our previous result $\gamma_1 = 0.88 \pm 0.1$ does not seem to need modification. Moreover, even for $J_s \approx J_{sc}$, the series evaluation of $T_c(J_s)$ is not as sensitive as the exponent determination, and thus our value of J_{sc} is probably also reasonably accurate.

The possibility of realizing such a two-dimensional magnet experimentally makes the search for appropriate materials quite worthwhile. In general, of course, the exchange interaction is weakened rather than strengthened at the surface, so that special conditions would have to be created. The most promising method seems to be the deposition of magnetic atoms on the surface of a less magnetic crystal, but diffusion of these impurities into the bulk may be a major problem.

The more common case of a weakened surface exchange ($J_s < J$) is also of interest. For sufficiently strong antiferromagnetic interactions the mean-field theory predicts a transition to a state of surface *antiferromagnetism*. We have not gone beyond mean-field theory in studying this case. In the more realistic case of a surface exchange J_s which is less than J but not negative enough to lead to antiferromagnetic order, there may be strong crossover effects which yield effective exponents differing from their true value. For example, we have calculated, using Monte Carlo techniques, the layer magnetization m_1 for a system of $55 \times 55 \times 20$ spins, with two free surfaces. We find that with $J_s = \frac{1}{2}J$, there is a large temperature region where the data fit an effective exponent $\beta_1^{eff} \approx 1$, even though the true exponent is undoubtedly $\beta_1 \approx \frac{2}{3}$. This effect could be used to interpret the experimental findings of Wolfram *et al.*⁴ The Ising model with modified surface exchange has also been studied in two-dimensions by Au-Yang,⁹ and the results are in qualitative agreement with our mean-field theory, with the important difference that there can be no surface ($d=1$) ordering at finite temperatures.

Our Monte Carlo calculations on Ising films also yield an estimate for the shift in T_c as a function of thickness. The data agree reasonably well with those of Allan¹⁰ and Fisher,¹¹ but extend to thicker films, and lead to a shift exponent^{11,12} $\lambda = \nu^{-1} \approx 1.5$. The previous calculation by one of us (K. B.) on hypercubes¹³ is argued to be consistent with this value, although the T_c shifts were so large there¹³ that the data were far from the asymptotic region of $\Delta T_c \rightarrow 0$, and they were thus also consistent with the value $\lambda = 1$ quoted in Ref. 13.

We have also carried out Monte Carlo calculations on a classical Heisenberg system with a free surface, which yield an exponent $\beta_1 \approx 0.75$ with rather large errors in the data. At low temperatures, the magnetization profile in the films is shown to agree quantitatively with the spin-wave calculations of Mills and Maradudin.¹⁴

In Sec. II the scaling theory of I is reviewed and generalized somewhat, and a number of new exponents and scaling relations are found. This theory is then "derived" from a cluster model, in much the same way as bulk scaling can be obtained from the cluster picture.¹⁵ Section III is devoted to a

discussion of numerical calculations on Ising and Heisenberg models, in order to test the sensitivity of the exponents found in I to the Hamiltonian. The exact results for the spherical model are also briefly discussed and compared with the scaling theory. In Sec. IV the Ising model with modified exchange ($J_s \neq J$) is studied both in mean-field theory and with high-temperature series. The criteria for surface ordering are found, and the exponents are calculated as a function of J_s . Section V contains a detailed summary of our results, and our conclusions.

II. GENERAL SURFACE SCALING AND CLUSTER MODEL

A. Scaling relations

In this section we wish to present a slightly more general formulation of surface scaling than in I, and to introduce a number of new exponents and scaling relations. We will then show that the surface scaling theory follows from a generalized cluster model, with an additional assumption on the shape of the clusters. We shall present our results using Barber's^{2,16} generalization of the scaling theory of I. For the moment we confine our attention to Ising-like models, all of whose properties are well defined below T_c . The modifications required for isotropic (Heisenberg and spherical) models will be discussed in Sec. III. We write the singular part of the free energy (per spin) of a d -dimensional system of n ($d-1$)-dimensional layers as

$$F(n, h, h_1, T) = n^\psi f(n^{-\varphi} h, n^{-\varphi_1} h_1, n^\theta |t|), \quad (2.1)$$

where h is a magnetic field acting on all the spins, h_1 is a field acting on the first and n th layers, and

$$t \equiv [T - T_c(n)]/T_c = t + \epsilon(n), \quad (2.2)$$

$$t = [T - T_c(\infty)]/T_c, \quad (2.3)$$

$$\epsilon(n) = [T_c(\infty) - T_c(n)]/T_c \approx bn^{-\lambda}, \quad n \rightarrow \infty. \quad (2.4)$$

From the definition of the bulk and surface¹⁷ free energies, F_b and F_s , we have

$$F(n, h, h_1, T) \approx F_b(h, t) + 2n^{-1}F_s(h, h_1, t) + \dots, \quad n \rightarrow \infty. \quad (2.5)$$

From the general scaling ansatz (2.1), we may write

$$F_b(h, t) = |t|^{2-\alpha} f_b(|t|^{-\Delta} h), \quad (2.6)$$

$$F_s(h, h_1, t) = |t|^{2-\alpha_s} \times f_s(|t|^{-\Delta} h, |t|^{-\Delta_1} h_1), \quad (2.7)$$

where

$$\psi = -(2-\alpha)\theta = -(2-\alpha_s)\theta - 1, \quad (2.8)$$

$$\varphi = -\Delta\theta, \quad (2.9)$$

$$\varphi_1 = -\Delta_1\theta, \quad (2.10)$$

and we have assumed¹¹ that

$$\lambda > 1. \quad (2.11)$$

Differentiating F_s with respect to h yields the "surface" magnetization m_s , and differentiating with respect to h_1 yields the "layer" magnetization¹⁸ m_1 , which has the form

$$m_1(t, h, h_1) = |t|^{\beta_1} \mathfrak{M}_1(|t|^{-\Delta} h, |t|^{-\Delta_1} h_1). \quad (2.12)$$

Then according to the definitions given previously,^{1,2}

$$\chi_s = \frac{\partial m_s}{\partial h} = \frac{\partial^2 F_s}{\partial h^2}, \quad (2.13)$$

$$\chi_1 = \frac{\partial m_1}{\partial h} = \frac{\partial^2 F_s}{\partial h \partial h_1} = \frac{\partial m_s}{\partial h_1}, \quad (2.14)$$

$$\chi_{1,1} = \frac{\partial m_1}{\partial h_1} = \frac{\partial^2 F_s}{\partial h_1^2}; \quad (2.15)$$

we may define the exponents $\gamma_s, \gamma_1, \gamma_{1,1}$, by

$$\left. \begin{aligned} \chi_1 &= \chi_1^0 |t|^{-\gamma_1}, \\ \chi_{1,1} &= \chi_{1,1}^0 |t|^{-\gamma_{1,1}}, \\ \chi_s &= \chi_s^0 |t|^{-\gamma_s}, \end{aligned} \right\} t \rightarrow 0, \quad h = h_1 = 0, \quad (2.16)$$

as well as $\beta_s, \beta_1, \delta_1, \delta_s$, and $\delta_{1,1}$,

$$m_s = m_s^0 (-t)^{\beta_s}, \quad t \rightarrow 0^-, \quad h = h_1 = 0, \quad (2.17)$$

$$m_1 = m_1^0 (-t)^{\beta_1}, \quad t \rightarrow 0^-, \quad h = h_1 = 0, \quad (2.18)$$

$$m_s \sim h^{1/\delta_s}, \quad h \rightarrow 0^+, \quad t = h_1 = 0, \quad (2.19)$$

$$m_1 \sim h^{1/\delta_1}, \quad h \rightarrow 0^+, \quad t = h_1 = 0, \quad (2.20)$$

$$m_1 \sim h_1^{1/\delta_{1,1}}, \quad h_1 \rightarrow 0^+, \quad t = h = 0. \quad (2.21)$$

Then the following scaling relations may be proved in the usual way, from the above equations:

$$\alpha_s = \alpha + \theta^{-1}, \quad (2.22)$$

$$\gamma_s = \gamma + \theta^{-1}, \quad (2.23)$$

$$\beta_s = \beta - \theta^{-1}, \quad (2.24)$$

$$2 - \alpha - \beta = 2 - \alpha_s - \beta_s = \Delta, \quad (2.25)$$

$$\beta_1 + \gamma_1 = \beta + \gamma = \beta_s + \gamma_s = \Delta, \quad (2.26a)$$

$$\beta_1 \delta_1 = \beta_s \delta_s = \Delta, \quad (2.26b)$$

$$\beta_1 (1 + \delta_{1,1}) = \beta_s (1 + \delta_s), \quad (2.27)$$

$$\gamma_1 (\delta_{1,1} - 1) = \beta_{1,1} (\delta_1 - 1), \quad (2.28)$$

$$\gamma_{1,1} + \beta_1 = \beta_{1,1} \delta_{1,1} = \Delta_1. \quad (2.29)$$

The equality of cross derivatives yields

$$\beta_1 + \Delta_1 = 2\beta_1 + \gamma_{1,1} = 2 - \alpha_s, \quad (2.30a)$$

$$\beta_s + \Delta = 2\beta_s + \gamma_s = 2 - \alpha_s, \quad (2.30b)$$

which can be combined with (2.29) and (2.26) to give

$$2\gamma_1 - \gamma_{1,1} - \gamma_s = 0. \quad (2.31)$$

Furthermore, from Eqs. (2.30), (2.29), and (2.22) we get

$$2 - \alpha_s = 2 - \alpha - \theta^{-1} = 2\beta_1 + \gamma_{1,1}. \quad (2.32)$$

Equation (2.23) with $\theta^{-1} = \nu$ was first obtained by Watson,¹⁹ and Eqs. (2.22), (2.24), and (2.25) are contained in Refs. 11 and 20. Equations (2.29), (2.30a), and (2.32) were derived by the authors in I, and Eqs. (2.26a), (2.30b), and (2.31) are due to Barber.² The remaining relations, involving β_s , δ_s , and δ_1 , are new. Moreover, it is clear that in principle only the assumption $\lambda > 1$ [Eq. (2.11)] is necessary to obtain these relations, and not the assumption

$$\theta = \nu^{-1} \quad (2.33a)$$

or

$$\lambda = \nu^{-1}. \quad (2.33b)$$

In the case¹¹

$$\lambda = 1, \quad \theta > 1, \quad (2.34)$$

θ^{-1} is replaced by 1 in Eqs. (2.22)–(2.24) and Eq. (2.30) does not hold, since the leading term in F_s is independent of h_1 .^{2,21} As pointed out by Barber² this invalidates Eq. (2.32). Such a situation arises in the spherical model for $d \geq 4$, as discussed in Sec. III C. Thus if in three dimensions the value $\beta_1 \approx \frac{2}{3}$ is obtained for the Ising model, this constitutes a test of the scaling relations, Eqs. (2.32) and (2.33a).

B. Cluster model

For bulk systems it is possible to “derive” the scaling relations from a simple cluster picture.¹⁵ This is done by writing the number of clusters of l -reversed spins in a field h , as

$$n_l \propto \exp\{-[a|t|l^\sigma + hl + \tau \ln l]\}, \quad (2.35)$$

where t is the reduced temperature (we consider only $t < 0$), a is a constant, and σ and τ are unknown exponents. The quantity l^σ represents the mean surface area of the cluster and the $\ln l$ term is a somewhat *ad hoc* representation of the main corrections to the “cluster free energy” for large l . The magnetization of a cluster is proportional to ln_l , and the mean magnetization of the whole system is

$$m = 1 - 2 \sum_{l=0}^{\infty} ln_l. \quad (2.36)$$

Inserting Eq. (2.35) and changing the sum to an integral we find

$$m_b = |t|^{(\tau-2)/\sigma} \mathfrak{M}_b(|t|^{-1/\sigma} h), \quad (2.37)$$

which is of the form (2.12), with

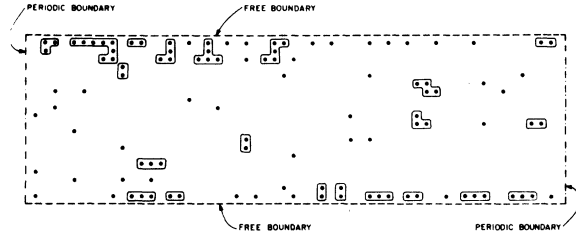


FIG. 2. Monte Carlo calculation of a typical spin configuration for a cross section of $55 \times 55 \times 20$ Ising film with two free boundaries, at $T = 0.63T_c$. Clusters of overturned spins are surrounded by a solid line, and it is clear that these occur more frequently near the free surfaces.

$$\beta = (\tau - 2)/\sigma \quad (2.38)$$

$$\Delta = 1/\sigma. \quad (2.39)$$

When our system has a surface, we expect the probability of occurrence of clusters to be different at the surface and in the bulk. This is illustrated qualitatively in Fig. 2, which represents a typical spin configuration in a Monte Carlo calculation of an Ising model with two free surfaces (and periodic boundary conditions on the other surfaces). Whenever a group of at least two adjacent spins are overturned we designate this group as a cluster and have surrounded it with a solid line. From the figure it is clear that the clusters are more frequent near the free surfaces than in the bulk. We shall attempt to incorporate this fact by expressing the number of surface clusters (i.e., clusters that touch the free surface) as

$$n_l^s \propto \exp\{-[a|t|l^{\sigma_1} + hl + ch_1 l^{\sigma_1,1} + \tau_1' \ln l]\}, \quad (2.40)$$

where c is a constant. The cluster is assumed to have l spins in all, of which al^{σ_1} are on the surface of the cluster, and $cl^{\sigma_1,1}$ intersect the free surface of the system and interact with the field h_1 ; the exponent τ_1' is a correction analogous to τ in the bulk. The layer magnetization for the surface layer is

$$m_1 = 1 - 2c \sum_{l=0}^{\infty} l^{\sigma_1,1} n_l^s, \quad (2.41)$$

which upon changing to an integral becomes,

$$m_1 = |t|^{\beta_1} \mathfrak{M}_1(|t|^{-\Delta'} h, |t|^{-\Delta_1} h_1), \quad (2.42)$$

where

$$\beta_1 = (\tau_1' - \sigma_{1,1} - 2)/\sigma_1, \quad (2.43)$$

$$\Delta' = 1/\sigma_1, \quad (2.44)$$

$$\Delta_1 = \sigma_{1,1}/\sigma_1. \quad (2.45)$$

This expression is again of the scaling form of Eq. (2.12), except that the exponent Δ' is arbitrary, and not necessarily related to the bulk exponent Δ .

From Eq. (2.42) we may derive those scaling relations involving the local exponents β_1 , γ_1 , δ_1 , $\gamma_{1,1}$, and $\delta_{1,1}$, namely,

$$\beta_1 \delta_1 = \beta_1 + \gamma_1 = \Delta', \quad (2.46)$$

and Eqs. (2.28) and (2.29). If we integrate Eq. (2.42) with respect to h_1 to find F_s , we obtain in general an integration constant which is equal to the surface free energy for $h_1 = 0$, $F_s(h, h_1 = 0, t)$. Assuming that this quantity scales with the same exponents as the full F_s , we may then derive the other relations of Sec. II A, except those involving the bulk exponents α , β , γ , δ , and Δ . In particular, Eq. (2.31) is seen to hold in this case, but Eq. (2.32) reads

$$2 - \alpha_s = 2\beta_1 + \gamma_{1,1}, \quad (2.47)$$

without reference to α . If $F_s(h, h_1 = 0, t)$ has different scaling exponents from $F_s(h, h_1, t)$, then certain scaling relations do not hold, as for example in the four-dimensional spherical model, studied in Sec. III C.

The assumption that the exponent Δ' of Eq. (2.42) is different from the bulk exponent Δ , means that $\sigma \neq \sigma_1$ [cf. Eqs. (2.39) and (2.44)]. In that case the surface area of a cluster which touches the sample surface is, even asymptotically, different from that of a bulk cluster. Although this assumption yields a possible scaling formulation with surface exponents unrelated to the bulk exponents, it does not seem physically realistic. In particular, if the correlation length in the system is the same in the bulk and at the surface (as is the case in two dimensions²² and probably also in three dimensions¹), one would expect surface and bulk clusters to have similar shapes and surface areas, i. e.,

$$\sigma = \sigma_1. \quad (2.48)$$

Then

$$\Delta = \Delta', \quad (2.49)$$

and the scaling formulation of Sec. II A is recovered, provided the integration constant mentioned above is not anomalous. In that case the entire difference between surface and bulk clusters can be taken into account by the logarithmic correction $\tau_1' \ln L$, and the interaction with the field h_1 . If we insert the values of the exponents for the two- and three-dimensional Ising models into Eq. (2.45) we find¹ $\Delta_1^{2d} = \frac{1}{2}$, $\Delta_1^{3d} \approx \frac{5}{8}$, $\sigma_{1,1}^{2d} = \frac{8}{30}$; $\sigma_{1,1}^{3d} \approx \frac{1}{3}$. Thus the number of spins in a surface cluster which touch the sample surface ($\sim L^{\sigma_{1,1}}$) is of the order of a line segment in three dimensions, and considerably less in two dimensions, so that the exponent $\sigma_{1,1}$ does not have an obvious geometrical interpretation.

III. SURFACE EXPONENTS FOR DIFFERENT MODELS

As stated in Sec. I, there is some doubt, both experimentally⁴ and theoretically² about the scaling ansatz (2.7), which leads to the prediction¹ $\beta_1 \approx \frac{2}{3}$. Furthermore, it is of interest to test the sensitivity of the results to the particular model under consideration and to the method used. We have therefore performed numerical calculations on both Ising and Heisenberg models, and have obtained independent estimates of the magnetization profile near a free surface.

A. Ising model

We have performed a Monte Carlo study of finite Ising "films" with periodic boundary conditions on the four sides, and free boundary conditions on the other two ends.²³ The critical temperature $T_c(L)$ for each value of the thickness L was determined by extrapolating the mean magnetization of the film to zero. The results, for systems of size $55 \times 55 \times L$ with $L = 2, 3, 5, 10, \text{ and } 20$ are plotted in Fig. 3, along with the series results of Allan and Fisher,^{10,11} and the previous results¹³ by one of us on hypercubes with six free boundaries [in the last case L is the effective thickness of the hypercube (see Ref. 13)]. It is seen that for small enough values of $\Delta T/T$ the results are consistent with the value $\lambda = \nu^{-1}$ [Eq. (2.33)], but there is a substantial deviation for larger $\Delta T/T$, which led to the original observation¹³ that $\lambda^{\text{eff}} = 1$ for hypercubes with $2 \leq L \leq 12$. That this last result is probably due to the nonasymptotic character of the data is seen by replotting the same information in Fig. 4, as $[T_c(\infty) - T_c(L)]/T_c(L)$ vs $L^{-1/\nu}$, which leads to a

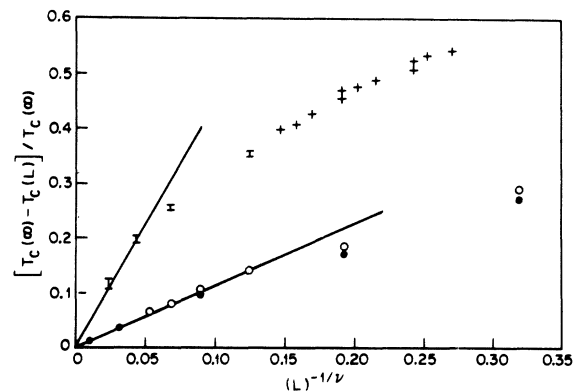


FIG. 3. Transition temperatures of Ising films of thickness L , plotted vs $L^{-1/\nu}$, to determine the shift exponent λ . The different symbols are I , Monte Carlo studies on hypercubes (Ref. 13); $+$, exact calculations for hypercubes (Ref. 13); O , series expansions by Allan and Fisher (Refs. 10 and 11); \bullet , this work. For small values of $\Delta T_c/T_c$ the data approach a straight line which goes through the origin, indicating that $\lambda = \nu^{-1}$.

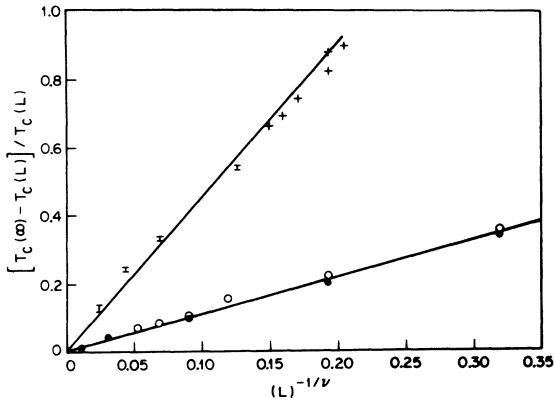


FIG. 4. Same data as in Fig. 3, but plotted as $[T_c(\infty) - T_c(L)]/T_c(L)$, rather than $[T_c(\infty) - T_c(L)]/T_c(L)$. The fit of the hypercubes and thinnest films to a straight line going through the origin is much better than in Fig. 3, indicating at the least that some of the data are not in the asymptotic region.

much better fit. Although the improved agreement with the relation $\lambda = \nu^{-1}$ is only suggestive, it does show that the apparent violation of this relation for hypercubes¹³ was probably due to the nonasymptotic nature of the $\Delta T/T$ data. We note the agreement between the Monte Carlo and series results on films, and we conclude that the present data on thicker films lend further support to the scaling conjecture^{11,12,24} $\lambda = \nu^{-1} \approx 1.5$. In particular, the

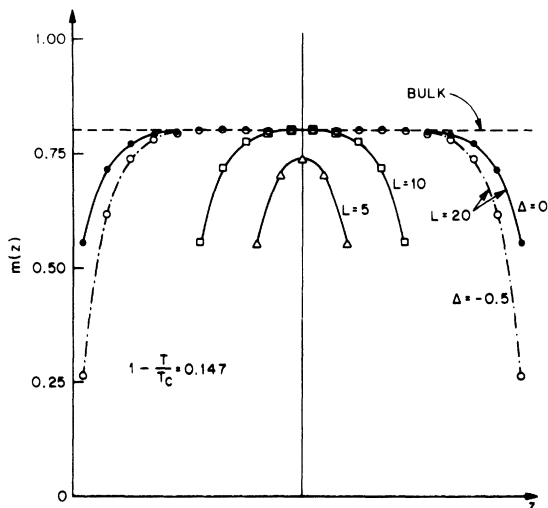


FIG. 5. Monte Carlo calculation of the magnetization of Ising films as a function of position for different thicknesses L . For all but the thinnest film the magnetization reaches its bulk value (for that temperature) at the center, denoted by a dashed line. Thus the film results are appropriate for a semi-infinite system as well. The open circles show the effect of a weakened surface exchange on the magnetization [$J_s = J(1 + \Delta) = \frac{1}{2}J$].

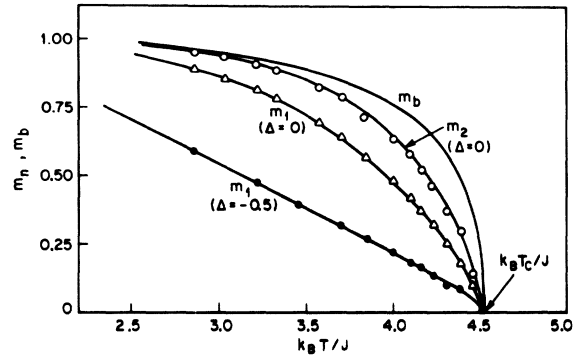


FIG. 6. Monte Carlo results for the magnetization of the Ising model as a function of temperature for different layers. The curve marked $\Delta = -0.5$, corresponding to a weakened surface exchange, is consistent with an effective exponent $\beta_1^{\text{eff}} \approx 1$ over a considerable temperature range, even though there is a crossover to a lower value of β_1 very near T_c .

alternative conjectures of Fisher and Ferdinand²⁰ and of Domb,²⁰ that $\lambda < \nu^{-1}$, have no basis in the present data.

Our numerical calculations also yield information on the spatial distribution of the spontaneous magnetization in Ising films, and on its temperature dependence. Figure 5 shows, as an example, the magnetization profile for $(T_c - T)/T_c = 0.147$, in films of different thicknesses. Except for the thinnest film ($L = 5$), the magnetization reaches its bulk value in the middle, so that these films are adequate for a study of the semi-infinite system, at least for T not too near T_c . The "bulk" magnetizations agree with each other for the various film thicknesses, and with the Padé approximants of Baker,²⁵ thus providing a check on the numerical

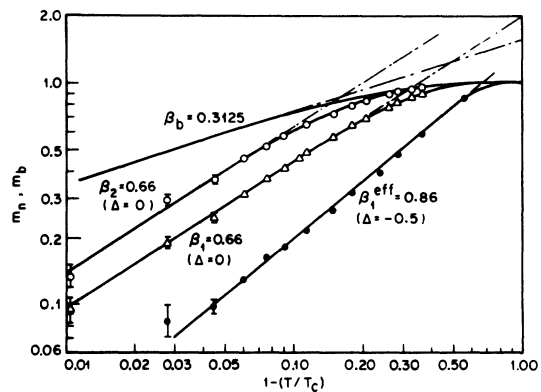


FIG. 7. Same data as in Fig. 6, plotted on a log-log scale, displaying the exponent $\beta_1 \approx \frac{2}{3}$. For $\Delta = -0.5$ the exponent is $\beta_1^{\text{eff}} = 0.86$, with T_c fixed at its bulk value, but if T_c is allowed to vary, then a slightly higher β_1 gives a better fit.

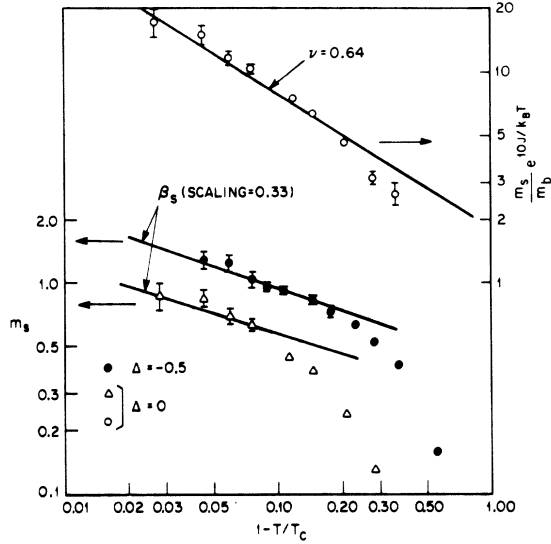


FIG. 8. Surface magnetization [defined in Eq. (3.1)], for Ising films, as a function of temperature (left-hand scale), compared with the scaling prediction $\beta_s = -0.33$. The scaling theory is tested directly by comparing m_s/m_b with the bulk correlation length ξ on the upper curve (right-hand scale). The data have been multiplied by the function $e^{10J/k_B T}$, which is regular near T_c but is constructed to cancel out some of the low-temperature corrections.

methods. The temperature dependence of the magnetization is shown in Fig. 6, on a linear scale, for the first and second layers, with subsequent layers omitted, but approaching the bulk value uniformly. (The curves in Figs. 5–7 labeled $\Delta = -0.5$ will be discussed in Sec. IV D.) The same results as in Fig. 6 are plotted on a log-log scale in Fig. 7, where the exponent $\beta_1 = 0.66$ is shown for the first layer, in the reduced temperature region $10^{-2} \leq 1 - T/T_c \leq 2 \times 10^{-1}$. This exponent agrees remarkably well with the scaling prediction $\beta_1 = 0.64 \pm 0.08$ given in Eq. (6.14) of I. The exponent β_2 for the second layer is also consistent with the value 0.66, but the magnetization breaks away from its asymptotic dependence, in a typical crossover toward the bulk behavior. The effect is of course stronger for the layers which are further from the surface.

It is also possible to compute the surface magnetization,

$$m_s \equiv \frac{\partial F_s}{\partial h}, \quad (3.1)$$

using the relation^{1,26}

$$m_s = \lim_{L \rightarrow \infty} \frac{1}{2} \sum_{n=1}^L (m_b - m_n). \quad (3.2)$$

The temperature dependence of m_s is shown in Fig. 8, and its exponent β_s is seen to be consistent

with the scaling estimate [Eqs. (2.24) and (2.33)] $\beta_s = \beta - \nu \approx -\frac{1}{3}$. A more direct test of scaling is obtained by showing that m_s/m_b is proportional to the bulk correlation length ξ . Since, however, for $T \rightarrow 0$ $m_b \sim 1 - 2e^{-12J/k_B T}$ and $m_1 \sim 1 - 2e^{-10J/k_B T}$, we have multiplied m_s/m_b by the term $e^{10J/k_B T}$ which is regular near T_c , but which is designed to remove the largest correction terms to the asymptotic behavior. The resulting plot is also shown in Fig. 8, and the agreement with the bulk correlation length exponent is reasonably good, within the rather large errors of the data. This plot also verifies, at least approximately, the exponential spatial dependence of the magnetization, with characteristic length ξ .

Finally, we show in Fig. 9 the ratios for the high-temperature-series expansion¹ of the layer susceptibilities χ_1, χ_2, χ_3 , and the bulk susceptibility χ_b , to illustrate the crossover from surface to bulk behavior. It is clear from this graph that the apparent exponent for χ_3 , say, cannot be the correct one, since a straight line through the last four points would intersect the ordinate at a completely incorrect value of T_c . We expect the points for χ_3 to merge with those for χ_1 , but this occurs for l values which are larger than those we calculate, corresponding to a crossover temperature close to T_c .

Let us conclude this section by summarizing the available information on the surface exponents for the three-dimensional Ising model. The value $\gamma_1 = \frac{7}{8}$ calculated in I, used in conjunction with the scaling relation² $\beta_1 + \gamma_1 = \beta + \gamma$, with $\beta = \frac{5}{16}$ and $\gamma = \frac{5}{4}$ yields $\beta_1 = \frac{9}{16}$, whereas the value $\gamma_{1,1} = 0$ of I, used with Eqs. (2.32) and (2.33a) gives²⁷ $\beta_1 = 0.62$ with $\alpha = \frac{1}{8}$, $\nu = 0.64$. These estimates, with error bars ± 0.1 are fully consistent with the Monte Carlo

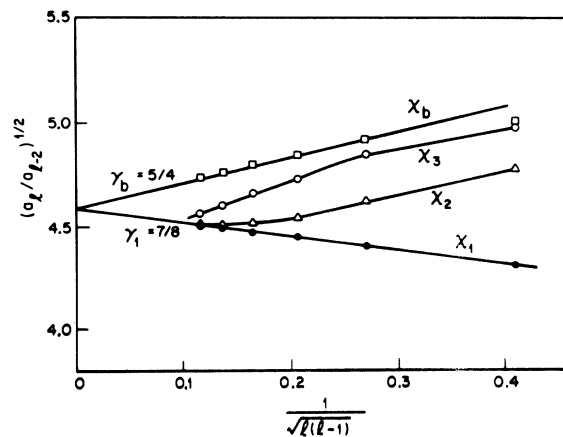


FIG. 9. Ratio plot of the high-temperature-series expansion for the layer susceptibility χ_n , showing the crossover from bulk to surface behavior.

value $\beta_1 = 0.66$ of Fig. 7 for the simple cubic lattice, but inconsistent with Barber's preliminary estimate² from a low-temperature series $\beta_1 = 1 \pm 0.12$. More recently, Barber has obtained⁵ $\beta_1 = 0.72 \pm 0.03$ for the fcc lattice, which overlaps the scaling and Monte Carlo results. It must be remembered, however, that even for the bulk, low temperature series are often quite unreliable, since they show seemingly spurious lattice dependences,²⁸ so the quoted errors⁵ seem to us rather optimistic. Using the values $\beta_1 = 0.64$, $\alpha = \frac{1}{8}$, and $\nu = 0.64$ in Eq. (2.30a) we obtain $\Delta_1 = 0.6$, and $\gamma_{1,1} = -0.04$. On the other hand, the value $\Delta_1 = \frac{1}{2}$ conjectured by Barber⁵ and Fisher,¹⁶ yields $\beta_1 = 0.735$ and $\gamma_{1,1} = -0.235$. This latter value seems unlikely to us, since it is difficult to reconcile with the direct series evaluation of $\gamma_{1,1}$ given in I. Thus at the present time we are inclined to prefer the values $\Delta_1 = \frac{2}{5} \sim \frac{3}{8}$ and $\beta_1 = \frac{2}{3}$, to the choice $\Delta_1 = \frac{1}{2}$, $\beta_1 = 0.72$, suggested by Barber⁵ and Fisher.¹⁶

Having checked that the scaling ideas put forward in I are reasonably consistent with the numerical data, we now turn to a study of the Heisenberg model, to see whether there might be noticeable deviations in this case.

B. Heisenberg model

Although we expect the bulk exponents for a Heisenberg model to be close to those of the Ising model, there are known to be differences between the two systems, and it is possible that these differences are magnified in the surface properties. For instance, it is possible that the scaling relation $\lambda = \nu^{-1}$ [Eqs. (2.33)] is violated in the Heisenberg system,²⁹ and that β_1 is quite different from $\frac{2}{3}$, thus explaining the experimental result⁴ referred to earlier. Moreover, at low temperatures, the existence of spin waves in the Heisenberg case strongly influences the thermodynamic properties, both in the bulk and near the surface. We have carried out Monte Carlo calculations to study some of these questions, and have found that the critical behavior is not severely modified, and that the low-temperature behavior is accurately described by spin-wave theory. Before discussing the numerical results we shall briefly review the spin-wave theory for finite and semi-infinite systems.

According to Mills and Maradudin¹⁴ the deviation of the magnetization in the n th layer from its bulk value is given by

$$\delta m_n = m_n - m_b = S \sum_{\mathbf{k}} \cos(2k_z n) \bar{n}(\Omega_{\mathbf{k}}), \quad (3.3)$$

where \mathbf{k} is a three-dimensional vector appropriate to the geometry of the sample, $\Omega_{\mathbf{k}}$ is the spin-wave frequency, and $\bar{n}(\Omega_{\mathbf{k}}) \equiv [\exp(\hbar\Omega_{\mathbf{k}}/k_B T) - 1]^{-1}$ is the occupation number. The bulk magnetization is given by

$$m_b = S - S \sum_{\mathbf{k}} \bar{n}(\Omega_{\mathbf{k}}). \quad (3.4)$$

Taking the classical limit, $\hbar \rightarrow 0$, $S \rightarrow \infty$, $\hbar S \rightarrow \text{const.}$ and normalizing the magnetization to unity at $T = 0$, we obtain $\bar{n}(\Omega) \propto T/\Omega$, and

$$\frac{m_n - m_b}{1 - m_b} = \frac{\sum_{\mathbf{k}} \cos(2k_z n) \Omega_{\mathbf{k}}^{-1}}{\sum_{\mathbf{k}} \Omega_{\mathbf{k}}^{-1}}. \quad (3.5)$$

The sums are over the Brillouin zone $-\pi \leq k_i \leq \pi$, in intervals of L_i^{-1} , where L_i is the i th dimension, and for a simple cubic lattice with unit lattice constant we take

$$\Omega_{\mathbf{k}} = A(3 - \cos k_x - \cos k_y - \cos k_z), \quad (3.6)$$

where A is a constant. For $n \rightarrow \infty$, and $L_i \rightarrow \infty$, we may convert the sums to integrals and we find

$$\frac{m_n - m_b}{1 - m_b} \sim n^{-1}, \quad (3.7)$$

with a coefficient independent of temperature. A more detailed evaluation of the spin-wave result will be described below, with reference to the specific system considered in our numerical calculations. It is interesting to note that Eq. (3.7) predicts a logarithmically divergent surface magnetization m_s , according to Eq. (3.2), so that the expansion in Eq. (2.5) does not seem to exist in the Heisenberg model in zero field below T_c . The modifications required in the scaling theory of Sec. II A will be discussed below with reference to the spherical model.

Our system was a cube of $16 \times 16 \times 16$ spins, with periodic boundary conditions on the four sides, a free boundary on one end, and "effective-field" boundary conditions on the other end. As shown in previous work by Müller-Krumbhaar and Binder,^{30,31} this boundary condition simulates bulk behavior, thus effectively making the system into a semi-infinite cylinder with a 16×16 cross section. The appropriate values for the effective field were taken from the results of Ref. 30. In Fig. 10, we show a typical cut through the system at a temperature $T = 0.77T_c$. The arrows are the projections of the magnetization in the y - z plane, both in direction and magnitude (in this classical system all spins have unit length). The average magnetization is assumed to point in the y direction. It is clear from the figure that near the free boundary the order has been considerably decreased, in comparison to its value at the other end of the sample, where the magnetization has its bulk value. This effect is shown quantitatively in Fig. 11, which is a plot of the average magnetization $\langle m(n) \rangle = m_y(n)$, as a function of the distance $n \equiv z + 1$ from the free surface, for different temperatures. As the temperature is raised toward T_c the effect of the free surface extends further and further into the bulk, and even at low temperatures the mag-

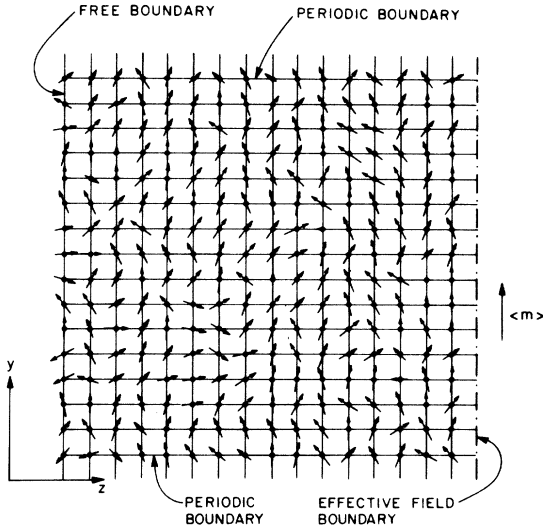


FIG. 10. Monte Carlo results for the cross section in the y - z plane of a $16 \times 16 \times 16$ classical Heisenberg spin system at $T = 0.77T_c$, with a free boundary at $z = 0$, an "effective-field boundary" simulating bulk behavior at $z = 16$ (see Ref. 30), and periodic boundary conditions on the other faces. The arrows at each site denote the y - z projection of the (unit) spin vector. The average magnetization points in the y direction, but its magnitude is clearly smaller near the free surface.

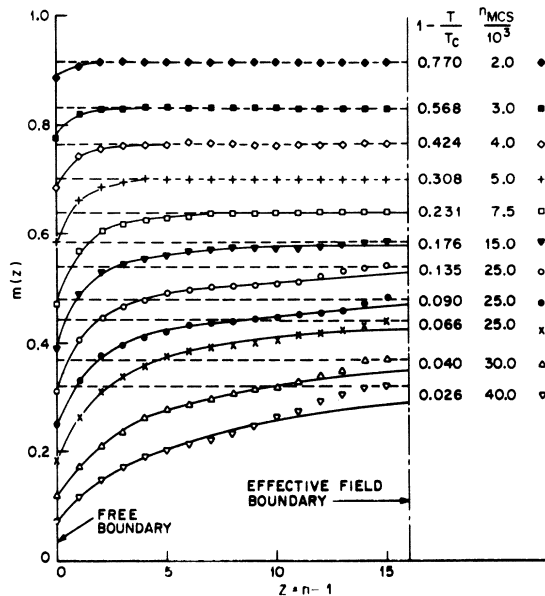


FIG. 11. Monte Carlo data for the magnetization profile in the Heisenberg system shown in Fig. 10 for various temperatures. The effective-field boundary condition at $n = 16$ forces the magnetization to its bulk value, thus leading to unphysical behavior for T near T_c and $n > 12$. (The dashed lines represent the bulk calculations of Refs. 30 and 31). The number of configurations used is also shown, in units of Monte Carlo steps per spin n_{MCS} .

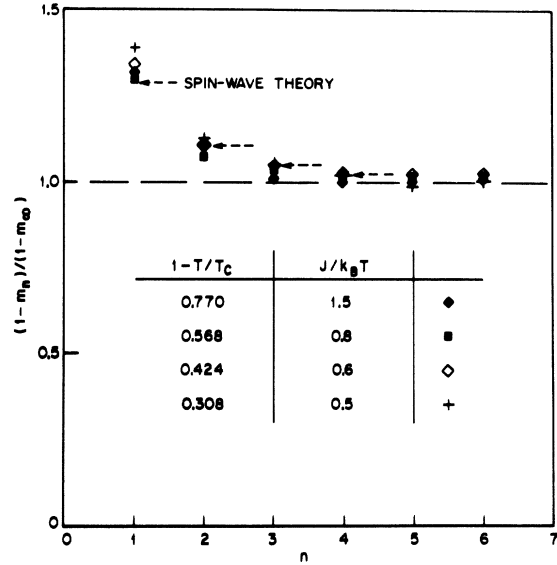


FIG. 12. Data of Fig. 11 are plotted again in a reduced form, to compare with the spin-wave theory given in Eq. (3.5). The agreement is seen to be well within the scatter of the numerical data, at least for $T/T_c < 0.6$.

netization does not reach its bulk value exponentially, as in the Ising model in Fig. 6, but rather according to a power law. Such a power law behavior is also expected for the analogous case of superfluid helium, thus invalidating the phenomenological theories,¹² even away from T_c . As mentioned earlier, the effective-field boundary condition forces the magnetization to have its bulk value at the 16th layer, so that at high temperatures the finiteness of the system leads to an artificially rapid variation of m for $n \geq 12$. The dashed lines in Fig. 11 represent the bulk values obtained from earlier Monte Carlo calculations,^{30,31} and the solid lines represent the expected behavior for a semi-infinite system.

In order to make a quantitative comparison of the data of Fig. 11 with the spin-wave theory,¹⁴ we have evaluated Eq. (3.5) for a system of size $16 \times 16 \times \infty$, which is periodic in the finite cross section, namely, we took finite sums over k_x and k_y [$k_{x,y} = j\pi/16, j = 1, \dots, 16$], and performed an integral over k_z . The results are shown in Fig. 12, where $[1 - m_n]/[1 - m_b]$ is plotted versus the distance n . It is seen that the temperature independence of this quantity predicted in Eq. (3.5) is quite well verified up to $T \approx 0.77T_c$, within the accuracy of the numerical data, and the quantitative agreement with Eq. (3.5) is excellent. Only the points at $n = 1$ and $1 - T/T_c = 0.308$ and 0.424 are outside the scatter in the data, and there finite-temperature corrections to spin-wave theory undoubtedly come into play. The spatial dependence

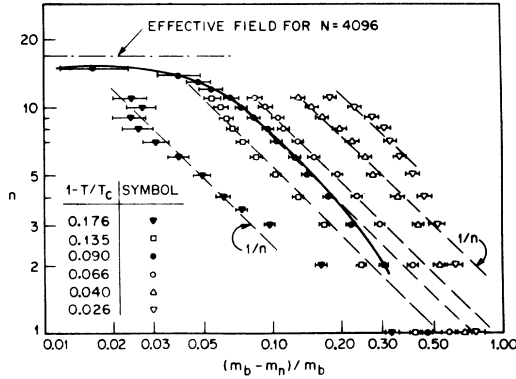


FIG. 13. Data of Fig. 11 are plotted on a log-log plot to show the $1/n$ dependence predicted by the spin-wave theory. Most of the points corresponding to large n have been omitted, since they are strongly perturbed by the finite size of the system. The solid line drawn through the data at $1 - T/T_c = 0.09$ is intended to illustrate this effect, and has no theoretical significance.

is shown again in Fig. 13, in a log-log plot of $(m_b - m_n)/m_b$ vs n , which shows the $1/n$ behavior of Eq. (3.7), for large n , at various temperatures. We have omitted the low-temperature data since the magnitude of $(m_b - m_n)/m_b$ is quite small and the errors in the calculation are relatively large; we have also omitted most points for $n \geq 12$, where the effective-field boundary condition has a strong perturbing effect (an example is given for the data at $T = 0.91T_c$). Finally, in Fig. 14 we show the layer magnetizations m_1 and m_2 as a function of temperature on a log-log plot. The behavior is quite similar to that of the Ising model (Fig. 7), with a slightly higher value of $\beta_1 (= 0.75 \pm 0.1)$, and fewer points close to T_c . In the temperature region $0.03 < (T_c - T)/T_c < 0.15$, however, which is the one studied in the low-energy-electron-diffraction (LEED) experiment,⁴ it is possible to exclude the value $\beta_1^{\text{eff}} = 1$ for the Heisenberg model. Thus we can surmise that the surface exponents of the Heisenberg model are close to those of the Ising model, and we must look elsewhere for an explanation of the data.⁴ Before turning to our study of modifications of exchange constants at the surface, we briefly review the available information on the spherical model.

C. Spherical model

The bulk properties of this model are anomalous²² below T_c , due to the divergence of the susceptibility as $h \rightarrow 0$, in three dimensions, and divergences in higher derivatives for $d \geq 4$. Thus there is an essential asymmetry between $T > T_c$ and $T < T_c$. Strictly speaking, of course, the scaling functions for Ising-like models discussed in Sec. II are also not functions of $|t|$, i. e., they may be different for $t > 0$ and $t < 0$. We have suppressed

this difference, however, since it does not affect the exponents, which are expected to be symmetric. For the spherical model, on the other hand, the asymmetry is significant, and one must introduce scaling functions which depend on the sign of t [e. g., in Eqs. (2.1)–(2.7) different functions f_b^+ , f_b^- , f_s^+ for $t > 0$ and $t < 0$, respectively]. In particular, for $d = 3$, the exponents γ , γ_s , γ_1 , α , and α_s are only defined above T_c , and the exponent β_s does not exist.³² Otherwise, this model has²¹ $\lambda = \nu^{-1} = 1$, and the homogeneity postulate (2.7) holds away from the coexistence curve ($h = 0$, $t < 0$), with different functions f_s^+ for $t > 0$ and $t < 0$, respectively. The critical exponents follow from the scaling relations of Sec. IIA (except those relations involving β_s), with $\alpha = -1$, $\Delta = \frac{5}{2}$, and $\Delta_1 = \frac{1}{2}$ (see Table I). For $d \geq 4$, there is another anomaly^{2,21} in the spherical model, namely, that $\lambda = 1$ and $\nu^{-1} = 2$. The other bulk exponents have their mean-field value (apart from logarithmic corrections for $d = 4$, which we neglect), i. e., $\alpha = 0$, $\Delta = \frac{3}{2}$. Thus²

$$F_s(h, h_1, t) = |t| f_{s1}^+(h/|t|^{3/2}) + |t|^{3/2} f_{s2}^+(h/|t|^{3/2}, h_1/|t|^{1/2}), \quad (3.8)$$

and the s -subscripted exponents, coming from the first term, behave anomalously. They are

$$\alpha_s = 1, \quad \gamma_s = 2, \quad \delta_s = -3, \quad \beta_s = -\frac{1}{2}. \quad (3.9)$$

It must be emphasized that just as for $d = 3$, these exponents may be undefined for $t < 0$, depending on the precise behavior of the function f_{s1}^- as its argument goes to 0. We have not studied this function in detail, but we note that β_s , in particular, may not exist for certain values of d . The other exponents are easy to find from Eq. (3.8), namely,

$$\beta_1 = 1, \quad \gamma_1 = \frac{1}{2}, \quad \delta_1 = \frac{3}{2}, \quad (3.10)$$

$$\gamma_{1,1} = -\frac{1}{2}, \quad \delta_{1,1} = \frac{1}{2}.$$

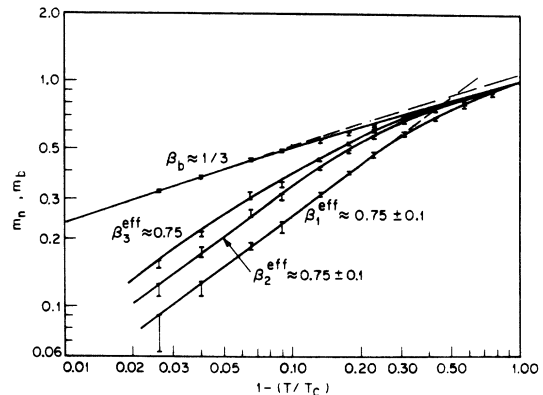


FIG. 14. Layer magnetization in the Heisenberg model as obtained from Fig. 11 on a log-log plot vs reduced temperature. The T_c value used is that of Ritchie and Fisher (Ref. 29), $J/k_B T_c = 0.3458$.

TABLE I. Spherical model.

	$d=3$	$d \geq 4$
α	-1	0
β	$\frac{1}{2}$	$\frac{1}{2}$
γ	2	1
δ	5	3
η	0	0
ν	1	$\frac{1}{2}$
α_s	0	1
β_s	a	$-\frac{1}{2}$
γ_s	3	2
δ_s	-5	-3
β_1	$\frac{3}{2}$	1
γ_1	1	$\frac{1}{2}$
δ_1	$\frac{5}{3}$	$\frac{3}{2}$
$\gamma_{1,1}$	-1	$-\frac{1}{2}$
$\delta_{1,1}$	$\frac{1}{3}$	$\frac{1}{2}$
η_1	1	1
η_{11}	2	2

^aNot defined.

These exponents satisfy the scaling relations (2.28), (2.29), and

$$\beta_1 \delta_1 = \beta \delta = \gamma_1 + \beta_1 = \gamma + \beta = \Delta, \quad (3.11)$$

but the equations relating s -subscripted exponents with others do not hold [e.g., (2.27), (2.30a), (2.32)].

When β_s is defined we have in addition the relations

$$(2 - \alpha_s) = \beta_s(\delta_s + 1) = \gamma_s + 2\beta_s. \quad (3.12)$$

The above values of γ_1 and $\gamma_{1,1}$ were quoted previously by Barber,² and α_s , γ_s , and δ_s were calculated by Watson³² [he denoted them as $\alpha(0)$, $\gamma(0)$, and $\delta(0)$, respectively].

The correlation exponents may be easily calculated from the pair correlation function given in Eq. (81) of Watson's review.³² We find for perpendicular correlations at T_c

$$C_{\perp}(z) \propto z^{1-d}, \quad (3.13)$$

from which¹

$$\eta_{\perp} = 1 = \eta_b + 1; \quad (3.14)$$

and for parallel correlations,

$$C_{\parallel}(\rho) \propto \rho^{-d}, \quad (3.15)$$

which implies

$$\eta_{\parallel} = 2 = \eta_b + 2. \quad (3.16)$$

These exponents satisfy the scaling law [cf. Eq. (5.27) of I]

$$\gamma_1 = \nu(2 - \eta_{\min}), \quad (3.17)$$

for both $d=3$ and $d \geq 4$. The spherical-model exponents are summarized in Table I.

The Heisenberg model is expected to behave similarly to the spherical model, namely, to satisfy a homogeneity postulate, with singularities on the coexistence curve. One consequence is the non-existence of a surface magnetization, for $h=0$, as already noted on the basis of spin-wave theory in Sec. IIIB.

IV. ISING MODEL WITH MODIFIED SURFACE EXCHANGE

Let us consider a semi-infinite Ising model with exchange interaction J between all nearest neighbors, *except* for spins in the surface layer, whose interaction is $J_s \equiv J(1 + \Delta)$ (the interaction between a surface spin and an interior spin is assumed to be J). Clearly, for very large values of J_s the surface behaves like a $(d-1)$ -dimensional Ising model and the bulk can be neglected, i.e., the two-dimensional surface will order ($d=3$), but not the one-dimensional surface ($d=2$). For $J_s = J$, the surface orders when the bulk does, and it is reasonable to assume that for $d=3$ there exists a critical value $J_{sc} \equiv J(1 + \Delta_c)$, above which the surface will order at a temperature $T_c(\Delta)$ which is higher than the bulk transition temperature $T_{c3}(J)$. We shall first study this problem using the mean-field theory.

A. Mean-field theory

According to the phenomenological theory discussed in Refs. 1 and 24 the existence of surface ordering depends on the sign of the extrapolation length λ , which is one of the parameters of the theory. A positive extrapolation length corresponds to $\Delta < \Delta_c$, whereas $\lambda < 0$ implies $\Delta > \Delta_c$. The temperature and spatial dependence of the magnetization for various values of λ were discussed in Refs. 1 and 24. In particular, for the case where the surface orders while the bulk is paramagnetic, the magnetization decays *exponentially* into the bulk, with a characteristic length equal to the bulk correlation length. As noted by Mills,⁷ this is not the situation envisaged by Sukiennicki and Wojtczak,⁶ so that their discussion cannot be used to rule out a state with surface ordering.

For our nearest-neighbor Ising model, the parameters T_c and λ may be expressed in terms of the microscopic Hamiltonian, following the method of Mills.³ The critical value $\Delta_c = \frac{1}{4}$ for surface

ordering and the extrapolation length $\lambda = (1 - 4\Delta)^{-1}$ were found by Mills³ and written in Sec. II B 2 of I. In Appendix A we solve the mean-field equations more completely, and derive the transition temperature $T_c(\Delta)$ and the susceptibility exponents. The results for the simple cubic lattice in three dimensions are

$$\left. \begin{aligned} T_c(\Delta) &= T_{c0} = 6J, \\ \gamma_1 &= \frac{1}{2}, \\ \gamma_{1,1} &= -\frac{1}{2}, \end{aligned} \right\} \Delta < \frac{1}{4}; \quad (4.1a)$$

$$\left. \begin{aligned} T_c(\Delta) &= T_{c0}(16\Delta^2 + 16\Delta + 1)/24\Delta, \\ \gamma_1 &= \gamma_{1,1} = 1, \end{aligned} \right\} \Delta > \frac{1}{4}; \quad (4.1b)$$

$$\left. \begin{aligned} T_c(\Delta) &= T_{c0}, \\ \gamma_1 &= 1, \\ \gamma_{1,1} &= \frac{1}{2}, \end{aligned} \right\} \Delta = \frac{1}{4}. \quad (4.1c)$$

These results are depicted in Fig. 15. The sudden change from "surface exponents" for $\Delta < \frac{1}{4}$ to bulk two-dimensional exponents for $\Delta > \frac{1}{4}$ is expected to lead to crossover effects, as explained in detail below.

In the case of antiferromagnetic surface exchange ($J_s < 0$) the surface layer behaves roughly like an Ising antiferromagnet in a (temperature-dependent) field.³³ At $T=0$ this field is uniform and equal to J , and the system makes a first-order transition from an antiferromagnetically ordered state ($m_1=0$), for $J < z_s |J_s|$, to a ferromagnetically ordered state for $J > z_s |J_s|$ (z_s is the number of nearest neighbors in the surface layer). At finite temperatures the transition on the surface becomes second order, in both the high- and low-temperature domains ($T \gtrsim T_{cb}$ and $T \rightarrow 0$, respectively). We have not solved the mean-field equation for intermediate temperatures (see Appendix B and Fig. 16).

When Mills first calculated³ the value of Δ_c , he expressed reservations about the validity of mean-field theory, since it completely neglects fluctuations. In an effort to clarify the situation we shall first discuss the exact solution of Au-Yang⁹ in two dimensions, and then present series expansion results in three dimensions.

B. Exact result for $d=2$

The work of McCoy and Wu²² has been generalized by Au-Yang⁹ to the case of arbitrary $J_s = J(1 + \Delta)$. Since the one-dimensional layer cannot order by itself, the transition temperature is independent of Δ . Moreover, the surface exponents were also found by Au-Yang to be independent of Δ , with only the coefficients being functions of Δ . Au-Yang calculated the layer magnetization as a function of Δ and T . At $T=0$ the surface behaves like a one-di-

mensional Ising antiferromagnet in a field J , caused by the aligned spins in the second layer. This system shows a first-order transition from an antiferromagnet to a ferromagnet with a *total* magnetization given by

$$m_1 = 0, \quad T = 0, \quad J < 2|J_s|, \quad J_s < 0 \quad (4.2a)$$

$$m_1 = 1/\sqrt{5}, \quad T = 0, \quad J = 2|J_s| \quad (4.2b)$$

$$m_1 = 1, \quad T = 0, \quad J > 2|J_s|. \quad (4.2c)$$

Equations (4.2a) and (4.2c) are the same as those found at $T=0$ in molecular field theory above. At finite temperatures there are deviations of order $e^{-8J/k_B T}$, but no antiferromagnetic order in the one-dimensional surface, unlike the prediction of mean-field theory. The full temperature and Δ dependence of m_1 is shown in Fig. 4 of Ref. 9. In three

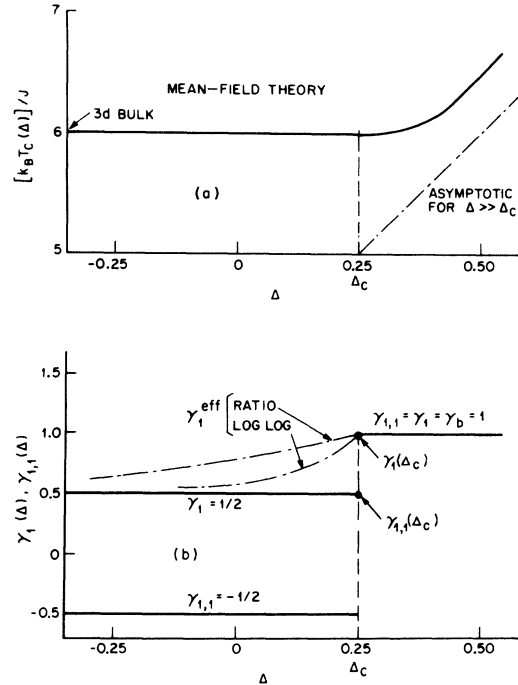


FIG. 15. (a) Transition temperature for the surface of an Ising model with exchange $J_s = J(1 + \Delta)$, calculated in mean-field theory and plotted vs Δ (J is the bulk exchange). For $\Delta < \Delta_c = \frac{1}{4}$ the surface orders at the bulk transition temperature, whereas for $\Delta > \Delta_c$ the transition in the surface occurs at a higher temperature $T_c(\Delta) > T_{cb}$. For very large Δ , $T_c(\Delta)$ becomes asymptotic to the two-dimensional transition temperature of the surface $T_c^{(2)} = 4J_s = 4J(1 + \Delta)$, denoted by the dot-dashed line. (b) Critical exponents γ_1 and $\gamma_{1,1}$ for the layer susceptibilities, plotted as a function of Δ , shown as heavy lines. A sharp crossover occurs at $\Delta = \Delta_c$, which is reflected in continuously varying effective exponents obtained from series expansions (ratio), or from fits to the susceptibilities over a finite temperature range (log-log). At $\Delta = \Delta_c$, $\gamma_1 = 1$ and $\gamma_{1,1} = \frac{1}{2}$.

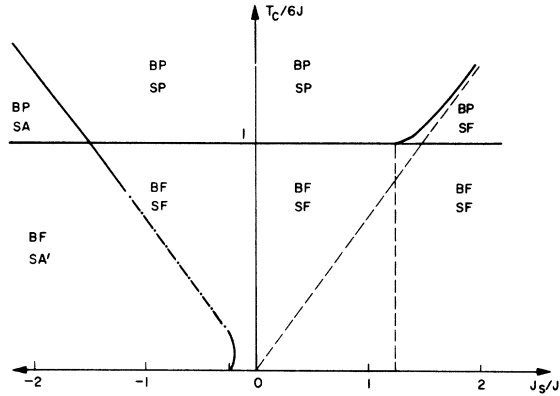


FIG. 16. A "phase diagram" comparable to that in Fig. 15a, but extended to negative values of J_s , calculated in mean-field theory. The nature of the surface and bulk order is indicated in each region by the symbols P for paramagnetic, F for ferromagnetic, and A and A' for antiferromagnetic, preceded by the symbols B for bulk and S for surface. In the state A' the surface spins have both a finite total magnetization and a finite staggered magnetization. Full curves denote second-order transitions, and the dot-dashed curve is the conjectured form of the transition line, obtained by a smooth extrapolation between the high- and low-temperature solutions (see Appendix B).

dimensions and for $T > 0$, it is expected that the system will follow the mean-field behavior more closely, since in contrast to the two-dimensional case,⁹ the surface *can* order independently of the bulk.

C. Series results for three dimensions

In an effort to determine the properties of a two-dimensional surface, we have carried out series expansions analogous to those in I, but for arbitrary values of $J_s = J(1 + \Delta)$. The correlation functions are represented in the form

$$C(\vec{r}', \vec{r}' + \vec{r}, t) = v^{l'm} \sum_{i=0}^{\infty} c_{i,m}(\vec{r}, \vec{r}', \Delta) v^i, \quad (4.3)$$

$$c_{i,m}(\vec{r}, \vec{r}', \Delta) = \sum_{m=0}^i c_{i,m}(\vec{r}, \vec{r}') \Delta^m, \quad (4.4)$$

where $v \equiv \tanh(2J/k_B T)$. It is to be noticed that $c_{i,1}$ (which occurs only if both \vec{r} and \vec{r}' are on the surface) is a coefficient of the two-dimensional Ising model, thus providing a welcome check on the calculation. The susceptibilities are then calculated just as in I. The values of the expansion coefficients of χ_1 , $\chi_{1,1}$, and χ_s are given in Tables II-V for $d=3$ (χ_1 coefficients are also listed for $d=2$). The ratio plots for χ_1 ($d=3$) for different values of Δ are shown in Figs. 17 and 18. From the intercept at $1/l \rightarrow 0$ we see that T_c is unchanged for $\Delta < \Delta_c$, where we may estimate

$$\Delta_c = 0.6 \pm 0.1, \quad (4.5)$$

and $T_c(\Delta)$ rises for $\Delta > \Delta_c$ [Fig. 18(a)].

A different plot of T_c vs Δ is given in Fig. 19, as an illustration of the similarity of the series and mean-field results.³⁴ From the slopes of the ratio plots we find an exponent γ_1 which seems to vary continuously with Δ for $\Delta < \Delta_c$, until it reaches the two-dimensional value $\gamma = \frac{7}{4}$ and then remains independent of Δ for $\Delta > \Delta_c$. A similar result is found for the exponent $\gamma_{1,1}$ of $\chi_{1,1}$. These continuously varying exponents, denoted as "effective exponents" are plotted in Fig. 20(b). In actual fact we believe them to be artifacts of our relatively short series (for reasons discussed below), and we believe that the true exponents experience a finite jump just as in the mean-field theory. Since, however, we wish to assert that our series *are* accurate enough to determine $T_c(\Delta)$, and in particular Δ_c reliably, we must examine our extrapolation procedures rather critically. Our conclusion will be that Eq. (4.5) gives a realistic estimate of the value of Δ_c , even though for $\Delta \lesssim \Delta_c$ the exponent is badly in error. Moreover, the series for $\Delta = 0$ are better behaved than for Δ finite, so that the exponents calculated

TABLE II. Series-expansion coefficients for the layer susceptibility χ_1 :

$$\chi_1 = \sum_{i=0}^{\infty} a_i(\Delta) v^i; \quad a_i(\Delta) = \sum_{m=0}^i a_{i,m} \Delta^m.$$

Table of $a_{i,m}$									
l/m	0	1	2	3	4	5	6	7	8
0	1								
1	5	4							
2	21	28	12						
3	93	152	120	36					
4	409	736	768	436	100				
5	1837	3508	4256	3340	1480	276			
6	8209	16396	21848	20692	12980	4716	740		
7	36969	76608	108936	116304	90392	47232	14544	1972	
8	166041	354900	531954	617584	522656	363552	162384	43348	5172

TABLE III. Ising 3d: Series-expansion coefficients for the surface susceptibility χ_s

$$\chi_s = \sum_{l=0}^{\infty} c_l(\Delta) v^l; \quad c_l(\Delta) = - \sum_{m=0}^l c_{l,m} \Delta^m$$

Table of $c_{l,m}$									
l/m	0	1	2	3	4	5	6	7	8
0	-1								
1	-1	4							
2	-10	32	12						
3	-71	200	132	36					
4	-440	1104	948	472	100				
5	-2553	5872	5876	3956	1580	276			
6	-14 126	30 080	33 424	26 952	14 960	4992	740		
7	-76 071	151 856	182 352	165 912	112 872	53 328	15 284	1972	
8	-399 868	752 200	962 724	957 704	747 862	440 644	180 810	45 320	5172

in I are expected to remain within the error limits quoted there (± 0.1).

The inaccuracy of the exponent value for $\Delta < \Delta_c$ (but $\Delta \neq 0$), may be seen from Fig. 17 (for $\Delta = 0.2$, say) by noticing that a straight line through the ratio points intersects the ordinate axis at a point corresponding to a temperature *below* T_{cb} . This result is clearly incorrect, since the interactions are entirely ferromagnetic and we must have $T_c(\Delta) \geq T_c(0)$ for $\Delta > 0$. The expected behavior in this range is for the points to follow the straight-line extrapolation until they reach the curve for $\Delta = 0$, and then to "change over" to the dependence corresponding to the exponent $\gamma_1(\Delta = 0)$. For $\Delta = \Delta_c \approx 0.6$, the straight-line extrapolation comes into T_{cb} and the effective exponent is $\frac{1}{4}$, corresponding to bulk two-dimensional behavior, and thereafter the effective exponent does not change, but the T_c value increases. For $\Delta > \Delta_c$ we expect no change-over, and the effective exponent is the real one [see Fig. 20(b)]. In determining Δ_c , we have assumed that for $\Delta > \Delta_c$, T_c depends linearly on $(\Delta - \Delta_c)$, whereas in general $T_c(\Delta)$ may have a

more complicated dependence (in mean-field theory it is quadratic) thus leading to a slightly different value of Δ_c . Our ignorance of this dependence is reflected in the error estimate quoted in Eq. (4.5).

A different method of data analysis is to calculate $\chi_1(T)$ from the series by Padé approximants, as shown on a log-log plot in Fig. 21. For $\Delta = 0.2$, for instance, there is a clear changeover from a $\gamma_1^{\text{eff}} = 1.5$ for $\Delta T/T_c > 4 \times 10^{-2}$, to a smaller exponent for $\Delta T/T_c < 4 \times 10^{-2}$. This latter exponent is not equal to the expected true exponent, because the Padé approximation is based on a small number of terms in the series, but it appears reasonable that with more terms the function would eventually curve over to a behavior characterized by $\gamma_1 \approx 0.9$. For $\Delta = -0.6$ the effective exponent is less than 0.9, and the curvature goes in the *other* direction, whereas for $\Delta = 0$ there is no perceptible curvature in the plot. The same is true for $\Delta > 0.6$, thus leading to the conclusion that the effective exponents for $\Delta \approx 0$ and $\Delta > \Delta_c = 0.6$ are the true ones, and the others are strongly affected by the changeover. The effective exponents γ_1^{eff} from both Padé and

TABLE IV. Ising 3d: Series-expansion coefficients for the local susceptibility $\chi_{1,1}$:

$$\chi_{1,1} = \sum_{l=0}^{\infty} a_l^{11}(\Delta) v^l; \quad a_l^{11}(\Delta) = \sum_{m=0}^l a_{l,m}^{11} \Delta^m$$

Table of $a_{l,m}^{11}$									
l/m	0	1	2	3	4	5	6	7	8
0	1								
1	4	4							
2	12	24	12						
3	40	108	108	36					
4	136	424	600	400	100				
5	516	1684	2864	2760	1380	276			
6	1968	6704	12 648	15 176	11 100	4440	740		
7	7904	27 700	55 324	75 724	70 292	41 412	13 804	1972	
8	31 484 ^a	114 936	240 416	357 968	387 992	293 736	144 816	41 376	5172

^aNote that this entry was incorrectly given in Table VII of I.

TABLE V. Ising $2d$: Series expansion coefficients for the layer susceptibility χ_1 :
$$\chi_1 = \sum_{l=0}^{\infty} a_l(\Delta) v^l; \quad a_l(\Delta) = \sum_{m=0}^l a_{l,m} \Delta^m.$$

Table of $a_{l,m}$											
l/m	0	1	2	3	4	5	6	7	8	9	10
0	1										
1	3	2									
2	7	6	2								
3	19	16	8	2							
4	49	44	24	10	2						
5	127	114	66	34	12	2					
6	321	304	188	102	46	14	2				
7	813	808	522	269	148	60	16	2			
8	2041	1994	1292	784	436	208	76	18	2		
9	5117	5032	3306	2064	1216	644	284	94	20	2	
10	12 763	12 658	8454	5390	3284	1860	928	378	114	22	2

ratio methods are shown in Fig. 20(b). The discrepancy between these determinations (≈ 0.07), even for $\Delta = 0$, is a measure of the inaccuracy of our knowledge of the true exponent. For $\gamma_{1,1}$, only the ratio method was employed, and the result is also shown in Fig. 20(b).

As a test of these ideas, we have carried out a similar analysis of the mean-field expression for χ_1 given in Eq. (A10) of Appendix A. Figure 22 is a log-log plot of χ_1 , which shows the change in effective exponent as Δ increases toward $\Delta_c = \frac{1}{4}$, and considerable curvature in the lines between $\Delta = 0$ and $\Delta = \Delta_c$ (since we are using the correct mean-field expression rather than a Padé approximant as in Fig. 21, the changeover is to the true exponent close to T_c). In Fig. 23 a ratio plot is given for eight terms of the high-temperature-series expansion of χ_1 [Eq. (A10)]. The linear extrapolations again cross the axis *below* the bulk T_c , showing that the effective exponents are not the true ones. In this case, even for $\Delta = 0$, the exponent and the T_c are incorrect, corresponding to deviations from the asymptotic behavior at $\Delta T/T = 5 \times 10^{-3}$ in the $\Delta = 0$ curve of Fig. 22. As Δ approaches Δ_c the extrapolated T_c and the effective exponent come closer to the true ones. The dependence of γ_1^{eff} on Δ in mean-field theory is shown in Fig. 15(b).

From the phenomenological theory of Refs. 1, 3, and 24, we may see that for $\Delta = \Delta_c$ the effect of the surface on the magnetization disappears, i. e., the magnetization is a constant throughout the system [$dm(z)/dz = 0$, for $z = 0$]. It is clear that the same will be approximately true in the real system. More precisely, it is likely that the average magnetization \bar{m} (integrated over z) just becomes equal to m_b when $\Delta = \Delta_c$, and that \bar{m} is larger than m_b for $\Delta > \Delta_c$, and smaller for $\Delta < \Delta_c$. From Eq. (3.2) it follows that the surface magnetization m_s vanishes at $\Delta \approx \Delta_c$.

The surface susceptibility χ_s has a particularly strange behavior as a function of Δ . For $\Delta \geq \Delta_c$, we have

$$\chi_s(\Delta) \simeq \chi_1(\Delta) \xi_b^{3d} \sim [T - T_c(\Delta)]^{-\gamma_b^{2d}} \times [T - T_c^{3d}]^{-\nu_b^{3d}}, \quad (4.6)$$

with $T_c(\Delta) > T_{cb}^{3d}$ for $\Delta > \Delta_c$. Thus we have

$$\gamma_s = \gamma_b^{2d}, \quad \Delta > \Delta_c \quad (4.7a)$$

$$\gamma_s = \gamma_b^{2d} + \nu_b^{3d}, \quad \Delta = \Delta_c \quad (4.7b)$$

whereas for $\Delta < \Delta_c$, the usual surface scaling applies [cf. Eqs. (2.23) and (2.33a)]

$$\gamma_s = \gamma_b^{3d} + \nu_b^{3d}. \quad (4.7c)$$

The high-temperature-series expansion will be

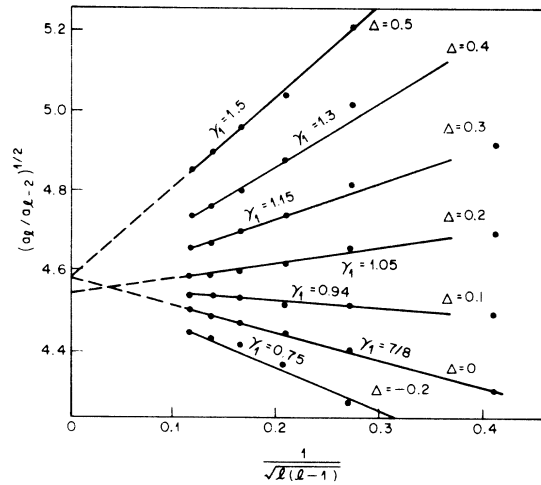


FIG. 17. Ratio plot for the high-temperature-series expansion of χ_1 , for different values of the surface exchange $J_s = J(1 + \Delta)$. The series for $\Delta \neq 0$ are seen to be unreliable since they extrapolate to a T_c value below the bulk (e.g., for $\Delta = 0.2$).

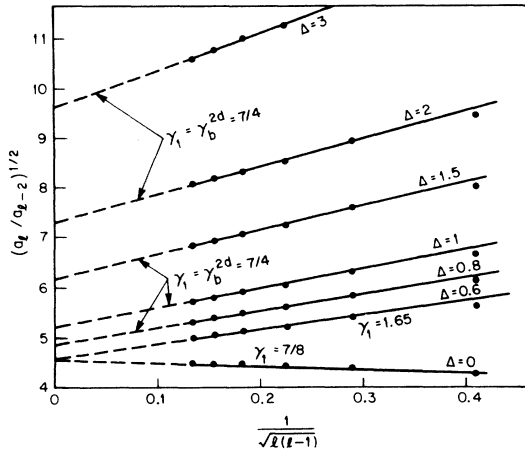


FIG. 18. Continuation of the plots in Fig. 17 for higher values of Δ . The plots are quite linear, and lead to higher T_c values than the bulk for $\Delta > \Delta_c \approx 0.6$, whereas the exponent remains at the bulk two-dimensional value $\gamma = \frac{7}{4}$.

particularly ill behaved, since the *sign* of χ_s changes at $\Delta = \Delta_c$, corresponding to the change in sign of m_s referred to above. Since χ_s always starts from unity at high temperatures, and its absolute mag-

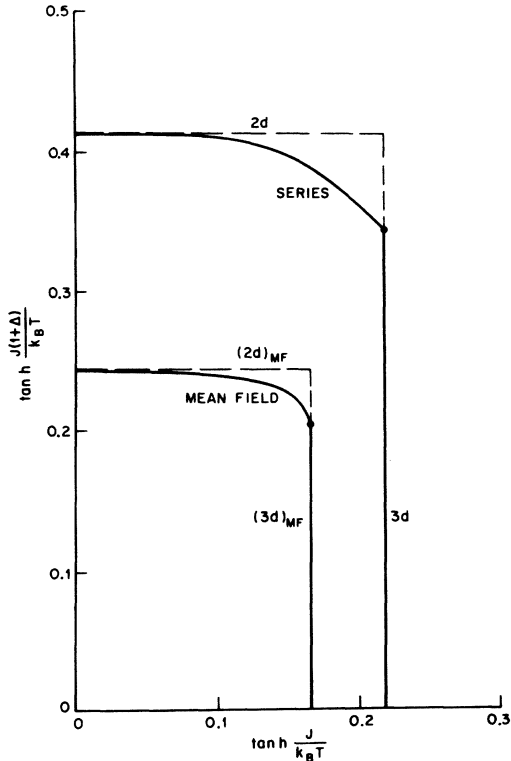


FIG. 19. Surface ordering temperatures of Figs. 15 and 17 replotted as $\tanh J(1+\Delta)/k_B T$ vs $\tanh J/k_B T$, showing the similarity of the mean-field and series results.

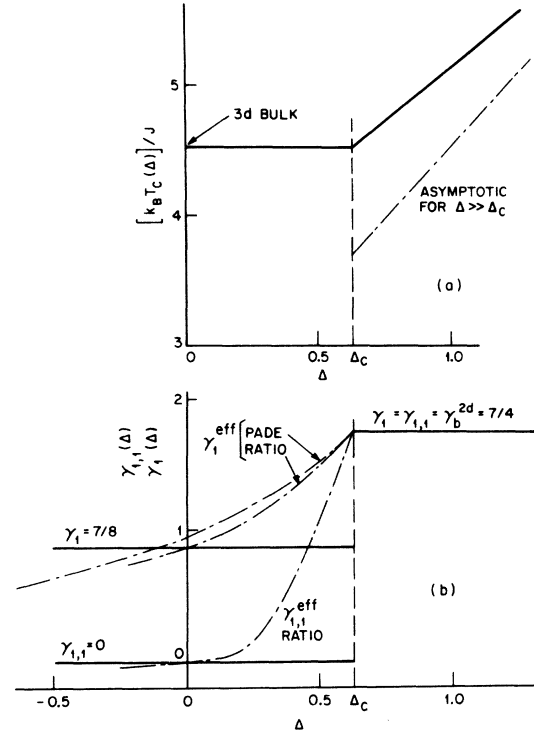


FIG. 20. An analogous plot to that in Fig. 15, except using the high-temperature series results. The critical value of Δ is seen to be $\Delta_c \approx 0.6$. The crossover of exponents is again accompanied by effective exponents which vary continuously with Δ .

nitude diverges at T_c , its behavior will be as shown schematically in Fig. 24(a). When a finite number of terms are used in the high-temperature series, the effective coefficient of the divergence, χ_s^0 , changes sign at a value $\Delta < \Delta_c$, and the effective ex-

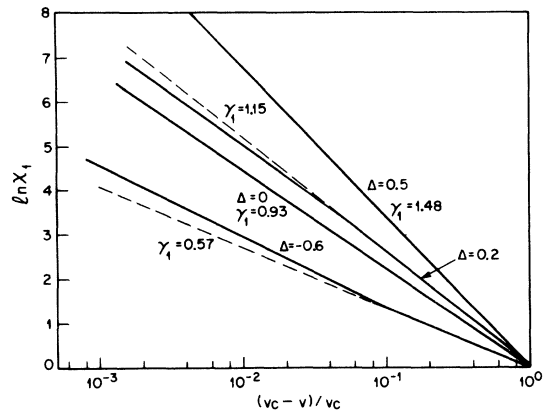


FIG. 21. Log-log plot of the (3,4) Padé approximants to some of the series in Fig. 19, plotted vs $(v_c - v)/v_c$ ($v = \tanh 2J/k_B T$) showing the curvature associated with the crossover. The curve for $\Delta=0$ has no curvature, and is presumed to yield the true exponent γ_1 . The (4,3) Padé approximants yield identical results.

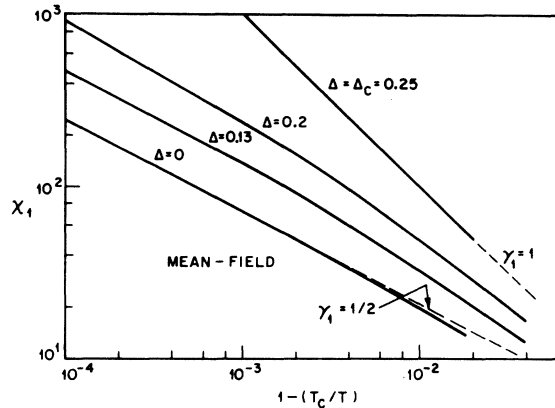


FIG. 22. Log-log plot of the layer susceptibility χ_1 , in mean-field theory, vs temperature for different values of Δ , showing the change of apparent exponent as $\Delta \rightarrow \Delta_c$.

ponents are quite meaningless near that value. These effective exponents, as derived from our series, are shown in Fig. 24(b), along with the "true" exponents of Eq. (4.7). It is seen that in the range $0 < \Delta < \Delta_c$ the behavior of the series is quite anomalous, whereas for $\Delta \geq \Delta_c$ the usual crossover behavior occurs.

D. Monte Carlo calculations for three dimensions

In an effort to simulate more realistic experimental situations, and to test the sensitivity of our Monte Carlo calculations to the parameter Δ , we have repeated the film computations described in Sec. III A, for $\Delta = -0.5$. This is shown as the dashed curve in Fig. 5, where the further weakening of the order at the surface is clearly visible (although Δ is negative it is not large enough in absolute magnitude to lead to antiferromagnetic

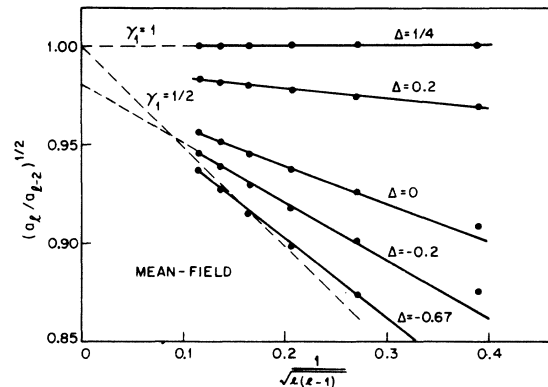


FIG. 23. Ratio plot of the high-temperature series for the mean-field layer susceptibility χ_1 . For no value of $\Delta < \Delta_c$ do the series extrapolate to the correct T_c , nor do they show the correct exponent ($\gamma_1 = \frac{1}{2}$).

ordering at the surface). The temperature dependence of the layer magnetization m_1 in this case is shown in Figs. 6 and 7. On the log-log plot of Fig. 7, with the T_c fixed at its bulk value, the effective exponent over the range $0.03 \leq \Delta T/T \leq 0.2$ is $\beta_1 = 0.86$, but the linear plot in Fig. 6 shows that when T_c is not known (as is the case in experimental situations), an exponent of $\beta_1 = 1$ fits the data quite well up to $\Delta T/T_c \approx 0.03$. The experiments of Wolfram *et al.*⁴ covered roughly the temperature range of the data in Fig. 6, so that a weakened surface exchange ($J_s \approx 0.5J$) is a possible explanation of their data. We expect of course that closer to T_c the exponent will change over to its scaling value $\beta_1 \approx \frac{2}{3}$.

V. CONCLUSION

We conclude by stating the principal results of this investigation.

- (i) The surface scaling theory^{1,2} has been further

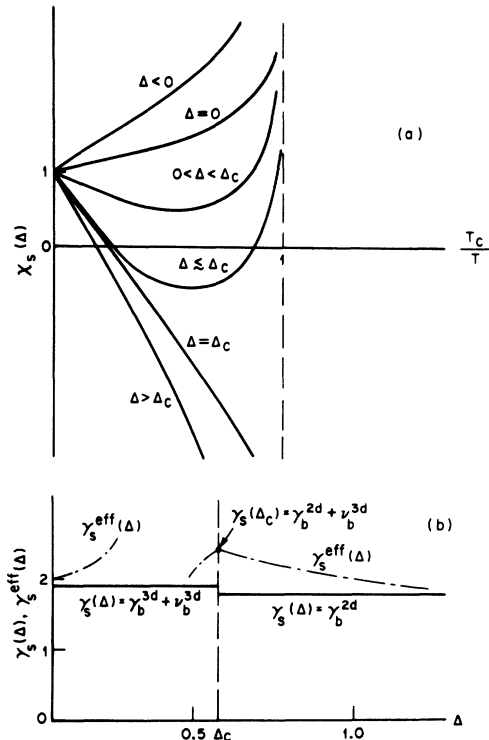


FIG. 24. (a) Schematic plot of the surface susceptibility χ_s as a function of temperature, for various Δ . Since χ_s is expected to change its sign near T_c as Δ goes through Δ_c , the behavior of the series will be quite irregular. (b) The exponent γ_s is plotted vs Δ , along with the effective exponents derived from series. Both the crossover at $\Delta = \Delta_c$ and the change in sign shown in part (a) for $\Delta < \Delta_c$ make the effective exponents quite erratic.

corroborated in Ising, Heisenberg, and spherical models. In the last two cases, however, the scaling functions have singularities as $h \rightarrow 0$ for fixed $T < T_c$, and a number of scaling relations fail to hold. The scaling theory follows from a cluster picture in which the probability for the appearance of a cluster is different near the surface and in the bulk. It may be noted that this generalized cluster model may be used to calculate nucleation rates near the surface (heterogeneous nucleation), in much the same way as one employs the usual cluster model for calculating homogeneous nucleation rates.³⁵

(ii) Monte Carlo calculations on Ising and Heisenberg models with free surfaces yield results consistent with scaling near T_c , and in the case of Heisenberg models, consistent with the spin-wave results of Mills and Maradudin¹⁴ at low temperatures. In particular, the prediction of I that the layer magnetization exponent β_1 for the Ising model should be 0.64 ± 0.08 is confirmed. In addition, the scaling assumption^{11,12} that the T_c shift exponent λ for films is equal to ν^{-1} also is correct for Ising systems in three dimensions.

(iii) A detailed study of the three-dimensional Ising model with modified exchange at the surface ($J_s \neq J$), shows that for $J_s > 1.6J$ the surface orders at a higher temperature than the bulk, and behaves like a two-dimensional Ising model above the bulk ordering temperature. The critical exponents experience a crossover at the critical value $J_{sc} = 1.6J$, and for $J < J_s \leq J_{sc}$ the series-expansion method yields extremely inaccurate exponents. Evidence for the existence of surface order above the bulk T_c has been reported by Højlund Nielsen³⁶ in the order-disorder transition of AuCu₃. A magnetic system where a similar effect could occur was suggested by Peschel and Fulde.³⁷ (See Note added in proof.)

(iv) For the case of weakened surface exchange ($J_s < J$), which would usually occur in practice, crossover effects also modify the effective exponents. Monte Carlo calculations for an Ising model in the case $J_s = \frac{1}{2}J$ show a large temperature region in which the layer magnetization m_1 has an effective exponent $\beta_1^{eff} = 1$, which is consistent with the experimental results of Wolfram *et al.*⁴ When the surface exchange is negative and sufficiently large in absolute magnitude, the surface can order antiferromagnetically, while the bulk is either paramagnetic or ferromagnetic (Appendix B).

Note added in proof. Recently, Weiner³⁸ has argued that surface ordering would occur in a Heisenberg system above the bulk transition temperature. This result seems highly implausible to us, for the same reason that a Heisenberg system of finite thickness does not order.³⁹ We wish to thank H. Fukuyama, B. Halperin, A. B. Harris, and C. Herring for discussions of this point.

ACKNOWLEDGMENTS

One of the authors (P. C. H) wishes to thank the members of the Theoretical Physics Department, Technical University, Munich, for their hospitality during the period when this paper was completed. The authors thank C. Domb, M. N. Barber, H. Au-Yang, and M. E. Fisher for discussions, and for sending them copies of their work prior to publication.

APPENDIX A: MEAN-FIELD THEORY WITH FERROMAGNETIC SURFACE EXCHANGE

Let us solve the mean-field equations³ for our system, and find the condition for an ordered state. These equations are

$$m_n = \tanh\left(\frac{H}{T} + \frac{z_s J}{T} m_n + \frac{J}{T} (m_{n+1} + m_{n-1})\right), \quad n \geq 2 \quad (A1)$$

$$m_1 = \tanh\left(\frac{H + H_1}{T} + \frac{z_s J_s}{T} m_1 + \frac{J}{T} m_2\right), \quad (A2)$$

where m_n is the magnetization in the n th layer, H is a uniform field acting on all spins, and H_1 acts only on the first layer. The quantity z_s is the number of nearest neighbors in each layer, and the exchange interaction is J , except between surface spins, where it is J_s .

Near T_c we can linearize Eqs. (A1) and (A2) and we find

$$m_n = \frac{H}{T} + \frac{z_s J}{T} m_n + \frac{J}{T} (m_{n+1} + m_{n-1}), \quad n \geq 2 \quad (A3)$$

$$m_1 = \frac{H + H_1}{T} + \frac{z_s J_s}{T} m_1 + \frac{J}{T} m_2. \quad (A4)$$

The system may be solved by setting³

$$m_n = m_\infty + \delta e^{-\alpha(n-1)}, \quad (A5)$$

and we find (for $z_s = 4$, i. e., $d = 3$, and a simple cubic lattice)

$$m_1 = \frac{H_1}{T} \left(\frac{6t_0}{3t_0 - 2 - 4\Delta + [(t_0 - 1)(9t_0 - 3)]^{1/2}} \right) + \frac{H}{T} \left(\frac{t_0}{t_0 - 1} \right) \left(\frac{3t_0 - 3 + [(t_0 - 1)(9t_0 - 3)]^{1/2}}{3t_0 - 2 - 4\Delta + [(t_0 - 1)(9t_0 - 3)]^{1/2}} \right), \quad (A6)$$

where ($z = 6$)

$$J_s \equiv J(1 + \Delta), \quad t_0 \equiv T/zJ = T/T_c(\Delta = 0). \quad (A7)$$

For $\Delta < \frac{1}{4}$ the denominator in the large parentheses is positive for $t_0 > 1$, so the susceptibilities first diverge at $t_0 = 1$, namely,

$$T_c = zJ = T_c(\Delta = 0) = T_{c0}, \quad \Delta < \frac{1}{4}. \quad (A8)$$

In this case it is easy to verify that

$$\chi_{1,1} = \frac{\partial m_1}{\partial H_1} = \frac{6}{T_{c0}} \left(\frac{1}{1 - 4\Delta + [6(T - T_{c0})/T_{c0}]^{1/2}} \right),$$

$$T \geq T_{c0}, \quad \Delta < \frac{1}{4} \quad (\text{A9})$$

$$\chi_1 = \frac{\partial m_1}{\partial H} = \frac{\sqrt{6}}{T_{c0}} \left(\frac{1}{(1 - 4\Delta)[(T - T_{c0})/T_{c0}]^{1/2}} \right),$$

$$T \geq T_{c0}, \quad \Delta < \frac{1}{4}. \quad (\text{A10})$$

For $\Delta > \frac{1}{4}$, on the other hand, the denominators vanish at a shifted T_c equal to

$$T_c(\Delta) = T_{c0}(16\Delta^2 + 16\Delta + 1)/24\Delta, \quad \Delta > \frac{1}{4}. \quad (\text{A11})$$

In the limit of large Δ this answer goes to ($z_s = 4$, $z = 6$)

$$T_c(\Delta) \approx \frac{2}{3} T_{c0} \Delta = z_s J \Delta \approx z_s J_s, \quad (\text{A12})$$

which is the mean-field value of the transition temperature in the two-dimensional layer. The susceptibilities are

$$\chi_1 = \chi_1^0 (T - T_c)^{-1}, \quad T > T_c > T_{c0}, \quad \Delta > \frac{1}{4}, \quad (\text{A13})$$

$$\chi_1^0 = (3 + A)[3 + \frac{1}{2}A + 9/(2A)]^{-1}, \quad (\text{A14a})$$

$$A \equiv [(9T_c - 3T_{c0})/(T_c - T_{c0})]^{1/2}, \quad (\text{A14b})$$

$$\chi_{1,1} = \chi_{1,1}^0 (T - T_c)^{-1}, \quad T > T_c > T_{c0}, \quad \Delta > \frac{1}{4}, \quad (\text{A15})$$

$$\chi_{1,1}^0 = 6[3 + \frac{1}{2}A + 9/(2A)]^{-1}. \quad (\text{A16})$$

From Eqs. (A9)–(A15) we have the exponents

$$\left. \begin{aligned} \gamma_1 &= \frac{1}{2}, \\ \gamma_{1,1} &= -\frac{1}{2}, \end{aligned} \right\} \Delta < \frac{1}{4} \quad (\text{A16a})$$

$$\left. \begin{aligned} \gamma_1 &= 1, \\ \gamma_{1,1} &= 1, \end{aligned} \right\} \Delta > \frac{1}{4} \quad (\text{A16b})$$

$$\left. \begin{aligned} \gamma_1 &= 1, \\ \gamma_{1,1} &= \frac{1}{2}, \end{aligned} \right\} \Delta = \frac{1}{4}. \quad (\text{A16c})$$

The results for the critical temperature and the exponents as a function of Δ are shown in Fig. 15. From Eq. (A5) it is easy to show that for $\Delta < \frac{1}{4}$,

$$q \sim [6(T - T_{c0})/T_{c0}]^{1/2}, \quad T \rightarrow T_{c0}^+, \quad \Delta < \frac{1}{4}, \quad (\text{A17})$$

and for $\Delta > \frac{1}{4}$

$$q = -\ln[(6T_c - 4(1 + \Delta)T_{c0})/T_{c0}], \quad \Delta > \frac{1}{4}. \quad (\text{A18})$$

Thus the transition for $\Delta < \frac{1}{4}$ is indeed to a state with bulk ordering ($q^{-1} \rightarrow \infty$), whereas in the case $\Delta > \frac{1}{4}$ the order decays exponentially⁷ with a finite decay length given by the inverse of Eq. (A18).

APPENDIX B: MEAN-FIELD THEORY WITH ANTIFERROMAGNETIC SURFACE EXCHANGE

In this case we must allow, in our molecular field equations, for a nonuniform magnetization in each layer. We shall confine our discussion to a two-sublattice configuration. The mean-field equa-

tions are in zero field, with $J_s < 0$,

$$m_n^A = \tanh \left[\frac{z_s J}{T} m_n^B + \frac{J}{T} (m_{n+1}^A + m_{n-1}^A) \right], \quad \Delta \geq 2, \quad (\text{B1})$$

$$m_n^B = \tanh \left[\frac{z_s J}{T} m_n^A + \frac{J}{T} (m_{n+1}^B + m_{n-1}^B) \right], \quad n \geq 2, \quad (\text{B2})$$

$$m_1^A = \tanh \left(\frac{-z_s |J_s|}{T} m_1^B + \frac{J}{T} m_2^A \right), \quad (\text{B3})$$

$$m_1^B = \tanh \left(\frac{-z_s |J_s|}{T} m_1^A + \frac{J}{T} m_2^B \right). \quad (\text{B4})$$

Let us set

$$m_n^{A,B} = m_n + \delta_n^{A,B} \quad (\text{B5})$$

and linearize the above equations with respect to $\delta_n^{A,B}$, obtaining

$$\delta_n^A = \left[\frac{z_s J}{T} \delta_n^B + \frac{J}{T} (\delta_{n+1}^A + \delta_{n-1}^A) \right] (1 - m_n^2), \quad n \geq 2 \quad (\text{B6})$$

$$\delta_n^B = \left[\frac{z_s J}{T} \delta_n^A + \frac{J}{T} (\delta_{n+1}^B + \delta_{n-1}^B) \right] (1 - m_n^2), \quad n \geq 2 \quad (\text{B7})$$

$$\delta_1^A = \left(\frac{-z_s |J_s|}{T} \delta_1^B + \frac{J}{T} \delta_2^A \right) (1 - m_1^2), \quad (\text{B8})$$

$$\delta_1^B = \left(\frac{-z_s |J_s|}{T} \delta_1^A + \frac{J}{T} \delta_2^B \right) (1 - m_1^2), \quad (\text{B9})$$

$$m_n = \tanh \left(\frac{z_s J}{T} + \frac{J}{T} (m_{n+1} + m_{n-1}) \right), \quad n \geq 2 \quad (\text{B10a})$$

$$m_1 = \tanh \left(\frac{-z_s |J_s|}{T} m_1 + \frac{J}{T} m_2 \right). \quad (\text{B10b})$$

Setting

$$\eta_n = \delta_n^A - \delta_n^B, \quad (\text{B11})$$

we find

$$\left(\frac{T}{J} + z_s (1 - m_n^2) \right) \eta_n = (\eta_{n+1} + \eta_{n-1}) (1 - m_n^2), \quad (\text{B12a})$$

$$\left(\frac{T}{J} - z_s \frac{|J_s|}{J} (1 - m_1^2) \right) \eta_1 = \eta_2 (1 - m_1^2). \quad (\text{B12b})$$

Equations (B10) and (B12) are a coupled set of nonlinear difference equations which are in general difficult to solve. One would have to obtain first the local magnetization m_n from Eq. (B10), and then insert the answer into the linear set (B12). There are, however, two limiting cases where the solution may be obtained analytically, since the local magnetization has a particularly simple form. The first case is that of high temperatures, where the total magnetization m_n is zero. Since we are considering negative values of J_s , it is clear that a magnetization appears in the system only below $T_{cb} = zJ$. Thus $m_n = 0$ for $T \geq T_{cb}$, and we must solve the equations

$$\left(\frac{T}{J} + z_s\right)\eta_n = \eta_{n+1} + \eta_{n-1}, \quad n \geq 2 \quad (\text{B13a})$$

$$\left(\frac{T}{J} - z_s \frac{|J_s|}{J}\right)\eta_1 = \eta_2, \quad (\text{B13b})$$

which may be done by setting

$$\eta_n = \eta_0 e^{-\alpha n} \quad (\text{B14})$$

and eliminating q to obtain

$$\frac{T_N}{J} = \frac{1 + z_s^2(|J_s|/J + |J_s|^2/J^2)}{z_s(1 + |J_s|/J)} \quad (\text{B15})$$

Equation (B15) gives the transition temperature for a transition to a state of surface antiferromagnetism, when no bulk magnetization is present. For large values of $|J_s|$ we have

$$T_N \sim z_s |J_s|, \quad (\text{B16})$$

which is the mean-field result for the transition in the surface, when the bulk is completely absent. For finite $|J_s|$, Eq. (B15) predicts that $T_N > z_s |J_s|$, which means that the effect of the bulk is to enhance surface antiferromagnetism, when the bulk is itself paramagnetic. This effect is almost certainly an artifact of mean-field theory, and in any case the enhancement is numerically small at all temperatures.

When the bulk is ferromagnetic, we must in principle solve for the local magnetization m_n from Eqs. (B10) and then insert it into Eqs. (B12). However, for T just below T_{cb} , we know that m_n is small, so its effect on Eqs. (B12) may be negligible. In particular, it was shown in Sec. II of I,

that $m_n^2 \propto (T_{cb} - T)^2$ for n within a distance ξ_b of the surface, so we indeed expect that to leading order in $T_{cb} - T$ we may neglect m_n in Eq. (B12a). Thus Eq. (B15) is also expected to describe the transition for T immediately below T_{cb} .

The other region in which the local magnetization is known, is the low-temperature case, where the spins are aligned in all layers, in the ferromagnetic state. By analyzing Eqs. (B10) we may show that for sufficiently low temperatures we have

$$m_n = m_b = \tanh(zJ/T)m_b, \quad n \geq 2 \quad (\text{B17a})$$

$$m_1 = \tanh\left(\frac{J - 4|J_s|}{T}m_b\right). \quad (\text{B17b})$$

Using Eqs. (B17), we may again solve Eqs. (B12) to find, for $T \rightarrow 0$,

$$\frac{T_N}{J} \left| \ln \frac{T_N}{J} \right| = 2 \left(1 - z_s \frac{|J_s|}{J} \right). \quad (\text{B18})$$

At low temperatures the problem is analogous to that of an antiferromagnet in a uniform field,³³ with a similar singular point at $T=0$, where the antiferromagnetic transition is of first order.

The high- and low-temperature solutions are plotted in Fig. 16 as solid lines. For intermediate temperatures, $0 < T < T_{cb}$, the mean-field equations [(B10) and (B12)] are relatively difficult to solve, and we have not attempted it here. In Fig. 16 we show by a dot-dashed curve a smooth interpolation between the two limiting cases, but we cannot rule out more complicated behavior, such as a first-order transition.

* Part of this work was carried out while K. B. held a Post-Doctoral Fellowship at the IBM Zürich Laboratory, 8803, Rüschlikon, Switzerland.

¹K. Binder and P. C. Hohenberg, Phys. Rev. B **6**, 3461 (1972), referred to as I.

²M. N. Barber, Phys. Rev. B **8**, 407 (1973).

³D. L. Mills, Phys. Rev. B **3**, 3887 (1971).

⁴T. Wolfram, R. E. DeWames, W. F. Hall, and P. W. Palmberg, Surf. Sci. **28**, 45 (1971).

⁵M. N. Barber, J. Phys. C **6**, L262 (1973).

⁶A. Sukiennicki and L. Wojteczak, Phys. Rev. B **7**, 2205 (1973).

⁷D. L. Mills, Phys. Rev. B **8**, 4424 (1973); see also, R. A. Weiner, Phys. Rev. B **8**, 4427 (1973).

⁸This point was missed in Ref. 6, as pointed out by Mills (Ref. 7).

⁹H. Au-Yang, J. Math. Phys. **14**, 937 (1973).

¹⁰G. A. T. Allan, Phys. Rev. B **1**, 352 (1970); see also Ref. 11.

¹¹M. E. Fisher, in *Critical Phenomena*, edited by M. S. Green (Academic, New York, 1971), pp. 1ff.

¹²V. L. Ginzburg and L. P. Pitaevskii, Zh. Eksp. Teor. Fiz. **34**, 1240 (1958) [Sov. Phys.-JETP **7**, 858 (1958)]; Y. G. Mamaladze, Zh. Eksp. Teor. Fiz. **52**, 279

(1967) [Sov. Phys.-JETP **25**, 479 (1967)].

¹³K. Binder, Physica **62**, 508 (1972).

¹⁴D. L. Mills and A. A. Maradudin, J. Phys. Chem. Solids **28**, 1855 (1967); D. L. Mills, Comments Solid State Phys. **4**, 28 (1971); Comments Solid State Phys. **4**, 95 (1972).

¹⁵M. E. Fisher, Physics (N. Y.) **3**, 255 (1967).

¹⁶M. E. Fisher, J. Vac. Sci. Technol. **10**, 665 (1973).

¹⁷Note that the surface free energy F_s and the surface exponents $\alpha_s, \beta_s, \gamma_s \dots$ are denoted $F^x, \alpha^x, \beta^x, \gamma^x \dots$ in Refs. 2, 11, and 16.

¹⁸Unfortunately, in Ref. 1 we sometimes referred to the "layer magnetization" as the "surface magnetization" [e.g., Sec. VII (i)]. In the present paper we shall be consistent in our terminology.

¹⁹P. G. Watson, J. Phys. C **1**, 268 (1968).

²⁰M. E. Fisher and A. E. Ferdinand, Phys. Rev. Lett. **19**, 169 (1967); A. E. Ferdinand and M. E. Fisher, Phys. Rev. **185**, 832 (1969); C. Domb, J. Phys. A **6**, 1296 (1973).

²¹M. E. Fisher and M. N. Barber, Phys. Rev. Lett. **28**, 1516 (1972); and Ann. Phys. (N. Y.) **77**, 1 (1973).

²²B. M. McCoy and T. T. Wu, Phys. Rev. **162**, 436 (1967).

²³A more extensive discussion of the numerical work on films will be published separately by K. Binder [Thin Solid Films (to be published)]. This paper should be consulted for additional references on the Monte Carlo method.

²⁴M. I. Kaganov and A. N. Omelyanchuk, Zh. Eksp. Teor. Fiz. 61, 1679 (1971) [Sov. Phys.-JETP 34, 895 (1972)]; M. I. Kaganov, Zh. Eksp. Teor. Fiz. 62, 1196 (1972) [Sov. Phys.-JETP 35, 631 (1972)].

²⁵G. A. Baker, Jr., Phys. Rev. 124, 768 (1961); Phys. Rev. 129, 99 (1963); J. W. Essam and M. E. Fisher, J. Chem. Phys. 38, 802 (1963).

²⁶Note that Eq. (3.12) of Ref. 1 should read

$$\chi_s = \lim_{N_1 \rightarrow \infty} \frac{1}{2} \sum_{n=1}^{N_1} (\chi_b - \chi_n).$$

²⁷Equation (6.14) of I was obtained using $\gamma_{1,1} = \gamma^* = 0$, and the bulk scaling relation $3\nu = 2 - \alpha$, in Eqs. (2.32) and (2.33b), yielding $\beta_1 = \nu = 0.64$. This value would be consistent with scaling only with $\alpha < \frac{1}{2}$, whereas in the text we obtain β_1 directly, without using bulk scaling. Needless to say, these differences are not significant, since they are well within the expected errors of the series, which we estimate to be ± 0.1 .

²⁸C. Domb and A. J. Guttman, J. Phys. C 3, 1652 (1970).

²⁹D. S. Ritchie and M. E. Fisher, Phys. Rev. B 7, 480 (1973).

³⁰K. Binder, Phys. Lett. A 30, 273 (1969); H. Müller-Krumbhaar and K. Binder, Z. Phys. 254, 269 (1972).

³¹K. Binder and H. Müller-Krumbhaar, Phys. Rev. B 7, 3297 (1973).

³²(a) P. G. Watson, in *Phase Transitions and Critical Phenomena*, edited by C. Domb and M. S. Green (Academic, New York, 1972), Vol. II, p. 101; (b) see also G. S. Joyce, in Ref. 32(a), p. 375.

³³C. G. B. Garrett, J. Chem. Phys. 19, 1154 (1951).

³⁴This method of plotting was suggested to us by M. E. Fisher.

³⁵A. Eggington, C. S. Kiang, D. Strauffer, and G. H. Walker, Phys. Rev. Lett. 26, 820 (1971).

³⁶P. E. Højlund Nielsen, Phys. Lett. A 42, 468 (1973).

³⁷I. Peschel and P. Fulde, Z. Phys. 259, 145 (1973); I. Peschel, Z. Phys. 265, 245 (1973).

³⁸R. A. Weiner, Phys. Rev. Lett. 31, 1588 (1973).

³⁹P. C. Hohenberg, Phys. Rev. 158, 383 (1967); N. D. Mermin and H. Wagner, Phys. Rev. Lett. 17, 1133 (1966); G. V. Chester, M. E. Fisher, and N. D. Mermin, Phys. Rev. 185, 760 (1969).